UNIVERSITY OF TARTU
Faculty of Science and Technology
Institute of Technology

Ana Shahpazir

Activity of macrolides against uropathogenic Escherichia coli

Bachelor's Thesis (12 ECTS)

Curriculum Science and Technology

Supervisor(s):
Assoc. Prof., PhD Niilo Kaldalu

Tartu 2023

Activity of macrolides against uropathogenic Escherichia coli

Abstract:

Azithromycin is a macrolide antibiotic extensively used to treat several infections attributable to Gram-positive bacteria. Exceptionally, azithromycin has proven to be effective in clinical treatment of widespread chronic infections caused by Gram-negative bacterium, *Salmonella*. While the underlying mechanisms of azithromycin's activity against this Gram-negative bacterium remain enigmatic, its efficacy brings up the question of whether this macrolide can be used in treatment of other Gram-negative bacterial infections as well. The goal of this work was to investigate the possibility of utilizing azithromycin against uropathogenic *Escherichia coli*. For this purpose, we determined the minimum inhibitory concentration of azithromycin in conditions resembling intracellular infection sites. Additionally, we validated the use of four macrolide bioreporters that were based on the regulatory leader peptide coding sequence of the macrolide resistance gene, *ermCL*.

Keywords:

Macrolides, azithromycin, UPEC, bioreporter

CERCS: B230, Microbiology, bacteriology, virology, mycology

Makroliidide antimikrobiaalne aktiivsus uropatogeense Escherichia coli suhtes

Lühikokkuvõte:

Asitromütsiin on makroliidide rühma kuuluv antibiootikum, mida kasutatakse sageli Gram-positiivsete bakterite poolt põhjustatud haiguste raviks. Erandlikult kasutatakse seda edukalt ka *Salmonella*, Gram-negatiivse patogeeni poolt põhjustatud krooniliste nakkuste raviks. Põhjused, miks asitromütsiin on selle Gram-negatiivse patogeeni ravis efektiivne, vajavad selgitamist ja viivad mõttele proovida sama ravimit ka muude Gram-negatiivsete bakterite vastu. Selle töö eesmärk oli testida asitromütsiini efektiivsust uropatogeense *Escherichia coli* vastu. Selleks määrati asitromütsiini minimaalsed inhibeerivad kontsentratsioonid tingimustes, mis sarnanevad tingimustega rakusisestes nakkuskolletes. Lisaks iseloomustati nelja erinavat makroliidi bioreporterit, kus reportergeeni ees asus *ermCL* resistentsusgeeni liiderpeptiidi kodeeriv järjestus.

Võtmesõnad:

Makroliid, asitromütsiin, UPEC, bioreporter

CERCS: B230, Mikrobioloogia, bakterioloogia, viroloogia, mükoloogia

TABLE OF CONTENTS

TERMS, ABBREVIATIONS AND NOTATIONS

AMP – Ampicillin

ATP – Adenosine triphosphate

AZM – Azithromycin

BFP – Blue fluorescent protein

Ca-MHB – Cation-adjusted Mueller-Hinton medium

CHL – Chloramphenicol

CLR – Clarithromycin

CPEC – Circular polymerase extension cloning

DMEM – Dulbecco's Modified Eagle's Medium

DMSO – Dimethyl sulfoxide

dNTP – Deoxynucleoside triphosphate

EPI – Efflux pump inhibitor

ERM – Erythromycin

Erm(s) – Erythromycin-resistance-methyltransferase(s)

GFP – Green fluorescent protein

HEPES – 4-(2-hydroxyethyl)-1-piperazineethanesulfonic acid

IM – Inner membrane

IPTG – Isopropyl ß-D-1-thiogalactopyranoside

JOS – Josamycin

KAN – Kanamycin

KAT – Katushka

LB – Luria-Bertani broth

LPM – Low Phosphate, low Magnesium medium

MES – 2-(N-morpholino) ethanesulfonic acid

MIC – Minimum inhibitory concentration

MID – Midecamycin

MOPS – 3-(N-morpholino) propanesulfonic acid

NPET – Nascent peptide exit tunnel

OLE – Oleandomycin

OM – Outer membrane

ORF – Open reading frame

PAβN – Phenylalanyl arginyl β-naphthylamide

PBS – Phosphate-buffered saline

PCR – Polymerase chain reaction

PMBN – Polymyxin B nonapeptide

PTC – Peptidyl transferase center

RFP – Red fluorescent protein

ROS – Rosamicin

rpm – Revolutions per minute

RPMI – Rosewell Park Memorial Institute Medium

SOB – Super Optimal Broth

SOC – Super Optimal Broth with Catabolite repression

SOL – Solithromycin

TAE – Tris-acetate-EDTA

TEL – Telithromycin

TYL – Tylosin

UPEC – Uropathogenic *Escherichia coli*

UTI – Urinary tract infection

INTRODUCTION

With the advent of antibiotics, bacterial infections were anticipated to belong to the past. Nevertheless, this development led to the emergence of bacterial mechanisms to counter the action of antibiotics, irrespective of the chemical class of the antimicrobial drug. The extensive use of high antibiotic doses to control bacterial infections in human, animals, and agriculture has led to a looming antibiotic-resistance crisis that has not been experienced previously, marking the end of the golden era of antibiotics. Over time, pathogenic strains of bacteria have developed resistance to most, if not all, available antibiotics. Thus, controlling bacterial infections has become alarmingly challenging. However, the worldwide upsurge in antibiotic resistance is not accompanied by novel antibacterial drug discovery. Therefore, to tackle the challenges imposed in the resistance era, it is crucial to use the currently available antibiotics more efficiently.

Macrolides are a promising class of antibiotics that are used predominantly to manage and treat various Gram-positive bacterial infections, such as pneumonia and tonsillitis, in clinical practice. In addition to their antimicrobial activity, macrolides hold beneficial anti-inflammatory and immunomodulatory effects in patients with chronic pulmonary inflammatory disorders (Amsden, 2005). Moreover, a particular macrolide antibiotic, azithromycin is commonly used for the treatment of *Salmonella* infections.

Urinary tract infections are among the most widespread recurrent bacterial infections that require extended periods of antibacterial therapy. Thus, they are among the most significant contributing factors to the spread of antibiotic resistance.

In this work, we aimed to shed light on the possibility of using macrolides more against Gram-negative bacterial infections. Thus, we chose uropathogenic *Escherichia coli* (UPEC) as our research organism. To uncover the potential utility of macrolides against UPEC, we determined MIC values in various conditions that resemble intracellular infection sites. Furthermore, we validated various macrolide bioreporters based on fluorescent proteins that created the opportunity to detect the encounter of bacterial cells with the drug. For this, we measured the fluorescence signal exhibited by bacteria upon encountering the drug in bacterial population at altered ionic and pH conditions. Flow cytometry was performed to investigate the reporter expression at the single cell level.

1 LITERATURE REVIEW

1.1 Antibiotics

Antibiotics are substances that perturb vital biochemical processes in bacteria and hence lead to the inhibition of cell growth and division or cell death (Brown & Wright, 2016). There are several aspects by which antibiotics can be categorized. Depending on their mode of action, antibiotics can be sorted into two groups of bactericidal and bacteriostatic. Bacteriostatic antibiotics such as macrolides solely stop bacterial growth, whereas bactericidal drugs stimulate cell death by disrupting key functions of the bacterial cell. Antibiotics belonging to both bacteriostatic and bactericidal groups act by binding to a target in the bacterial cell, inducing malfunctioning of the targeted essential cellular pathways or enzymes (Cho et al., 2014).

Additionally, antibiotics can be classified by the spectrum of their activity. Broad-spectrum antibiotics, such as ampicillin, inhibit a broad range of Gram-positive and Gram-negative bacterial species and can therefore be used to treat a variety of infectious diseases (Coates et al., 2002). Narrow-spectrum antibiotics, on the other hand, exhibit selectivity towards a genus or species in particular. Fidaxomicin is an excellent example of a narrow-spectrum antibiotic that is selective for Gram-positive anaerobes and is clinically used to treat *C. difficile* infections (Melander et al., 2018).

Antibiotics target essential cellular components in bacterial metabolism and thereby disable the bacteria (**Figure 1**). The most successful antibiotics hit one of these three targets or pathways: the ribosome (consisting of the 50S and 30S subunits), cell wall synthesis, and DNA gyrase or DNA topoisomerase (Lewis, 2013). The ribosome, which is responsible for synthesizing all cellular proteins, is a prime target for antibiotics and many antibacterials inhibit cell growth by impeding ribosomal functions (Wilson, 2014). Amid this group of antibiotics are macrolides which have been medically used for six decades.

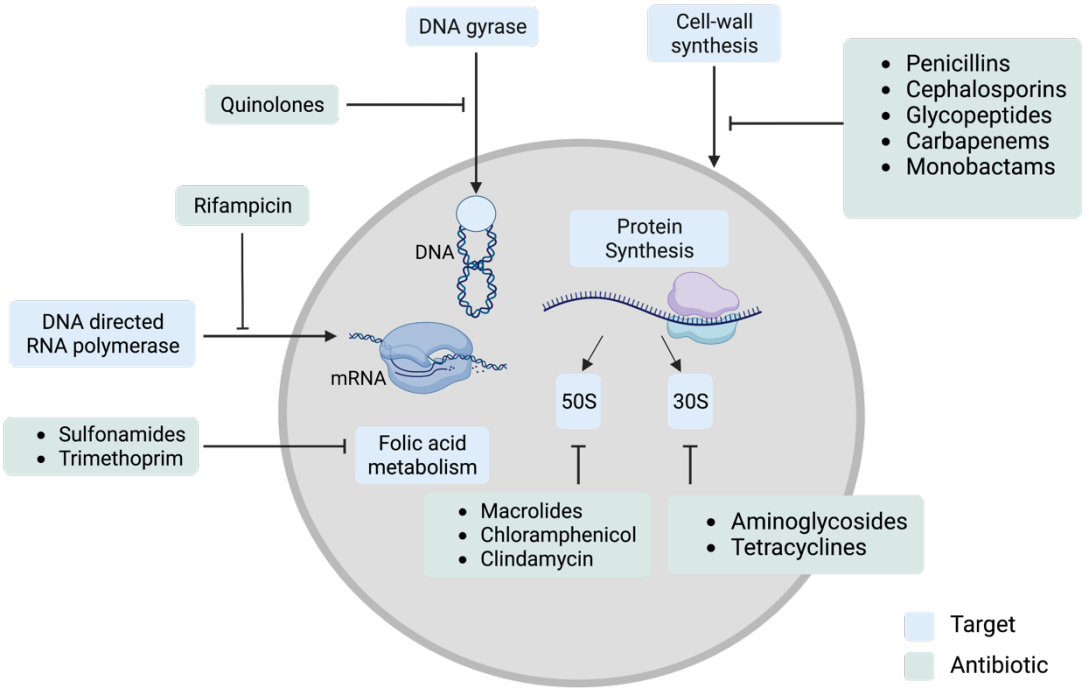

Figure 1. Antibacterial drug targets in bacteria. There are five main antibacterial drug targets in bacteria: protein synthesis (the ribosome), cell-wall synthesis, DNA gyrase, DNA-directed RNA polymerase, and metabolic enzymes. The figure shows the main antimicrobial drugs acting on these cellular components or pathways. These main antibiotics are Quinolones, Rifampicin, Sulfonamides, Trimethoprim, Macrolides, Chloramphenicol, Clindamycin, Aminoglycosides, Tetracyclines, Penicillins, Cephalosporins, Glycopeptides, Carbapenems, and Monobactams. Figure adapted from Lewis, 2013.

1.2 Macrolides

Macrolides are among the most successful and clinically essential antibiotics and are widely used for treating infections caused by Gram-positive bacteria (Gaynor & Mankin, 2005). Macrolides inhibit protein synthesis in bacterial cells by partially occluding the nascent peptide exit tunnel (NPET) located in the large subunit (50S) of the bacterial ribosome (**Figure 2**). NPET is a narrow channel through which the polypeptides assembled in the peptidyl transferase center (PTC) pass to exit the ribosome. It is known that the primary component of the macrolide binding site, in 50S ribosomal subunit, is constituted by RNA and numerous nucleotide residues in 23S ribosomal RNA (rRNA) bind to the macrolide molecule with high affinity (Vázquez-Laslop & Mankin, 2018).

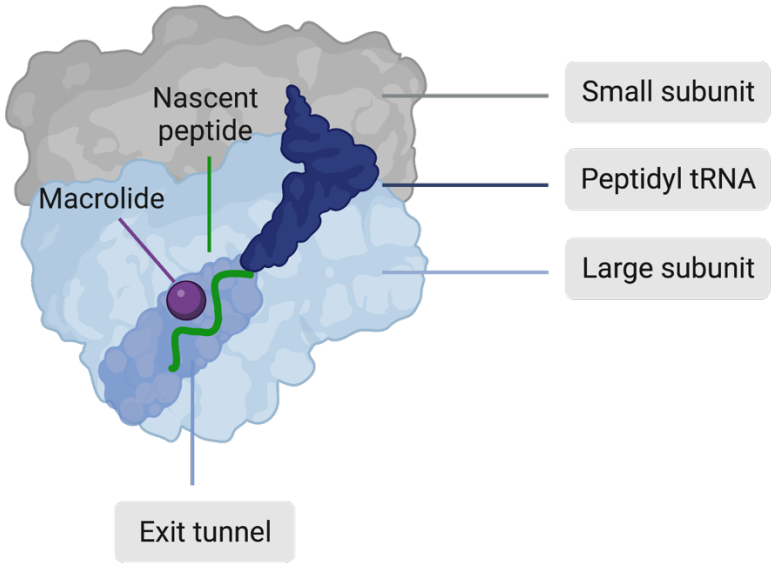

Figure 2. The macrolide binding site in the bacterial ribosome. The figure depicts the large subunit (50S) and small subunit (30S) of the bacterial ribosome. Macrolide antibiotics bind to the Nascent peptide exit tunnel (NPET) located in the large subunit and partially obstruct it, thereby inhibiting protein synthesis. Figure adapted from Ramu, Mankin and Vazquez-Laslop, 2009

Recent findings have depicted that while macrolides narrow the NPET significantly, they still leave sufficient room for the growth of the nascent protein chain, thus bringing up the possibility that some proteins might bypass the obstacle created by the drug. Therefore, macrolides can be considered highly selective translation modulators rather than global protein synthesis inhibitors. The context-specific action of macrolide antibiotics towards different polypeptide sequences is also apparent in vivo, as treating sensitive cells with very high concentrations of macrolides still allows to produce a group of cellular polypeptide chains (Kannan et al., 2014). Four modes of protein synthesis inhibition have been attributed to macrolides: 1) Inhibition of the progression of the nascent peptide chain during early translation (Mao & Robishaw, 1972); 2) Promotion of peptidyl tRNA dissociation from the ribosome (Menninger & Otto, 1982); 3) Inhibition of peptide bond formation (Mao & Robishaw, 1972); and 4) Interference with 50S ribosomal subunit assembly (Champney & Burdine, 1995). The high efficacy and safety of macrolides have rendered them clinically popular drugs, and their wide use has led to the inevitable emergence of resistant strains. Macrolide

resistance commonly occurs due to modification of the drug target site or excretion of the drug from the cell.

The most frequent mechanism of macrolide binding site modification is dimethylation of a single 23S rRNA nucleotide (A2058 in *E. coli*), which is located within the macrolide binding site, by erythromycin-resistance-methyltransferases (Erms). Dimethylation of A2058 excessively reduces drug affinity, rendering bacteria resistant to high concentrations of macrolide antibiotics. The expression of *erm* genes can be constitutive or inducible, and the molecular mechanisms of *erm* induction are highly relevant to the general mode of macrolide action. The inducible *erm* cassette contains two functional parts – the *erm* gene, whose expression is typically repressed and a constitutively translated leader peptide cistron that precedes *erm* (Weisblum, 1998). In the presence of an inducing macrolide antibiotic, the ribosome stalls around the 8^{th}-9^{th} codon of the leader peptide open reading frame (ORF). The ribosomal stalling triggers the rearrangement of the mRNA secondary structure, which makes the translation initiation region of the Erm cistron accessible and, thus, activates *erm* translation. On the contrary, in the absence of a macrolide or in too low macrolide concentrations, the stalling on the leader ORF will not occur. Hence, the *erm* gene will remain untranslated, as depicted in **Figure 3** (Gaynor & Mankin, 2005).

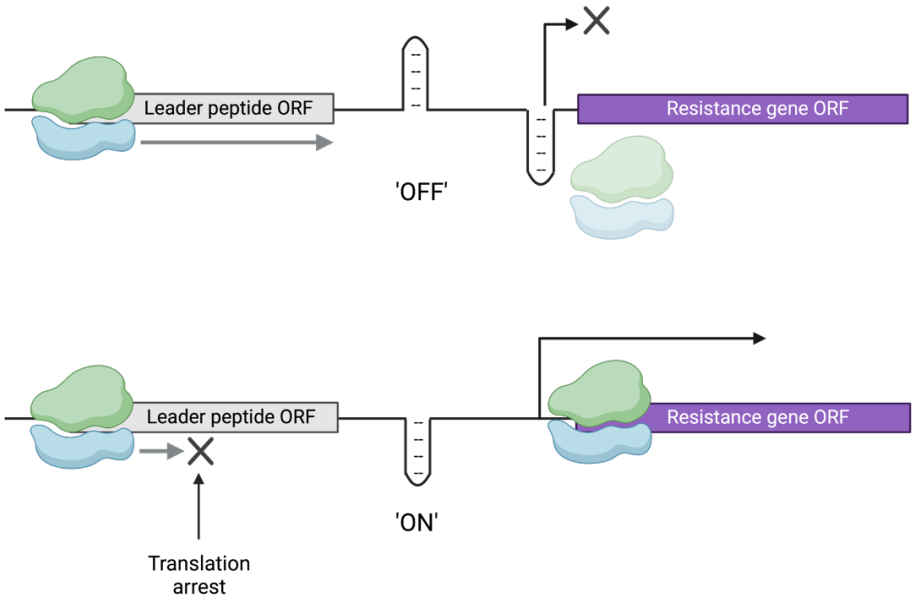

Figure 3. Inducible macrolide resistance operon. In an inducible macrolide resistance operon, a regulatory leader peptide open reading frame (ORF) precedes the resistance gene. In the absence of a macrolide antibiotic, the 'OFF' conformation of the intergenic region of

mRNA inhibits the ribosome from accessing the translation initiation site, and thus, the resistance gene is not expressed. On the contrary, in the presence of a macrolide, translation of the leader ORF is arrested at a specific codon and the structure of the mRNA is rearranged to 'ON' conformation, leading to the expression of the resistance gene. Figure adapted from Vázquez-Laslop and Mankin, 2018.

As the ribosomal stall on the leader ORF occurs only in the presence of the macrolide antibiotic, the ribosomes translating the leader peptide must bind a macrolide molecule. On the other hand, the ribosome translating the *erm* cistron should be drug-free at least in the early translational stages, to synthesize the entire polypeptide. This indicates that the efficiency of *erm* induction is critically dependent on macrolide concentration. At deficient drug concentrations, not enough ribosomes will carry the antibiotic, and thus the stalling on the leader peptide ORF will not take place. Alternatively, very high concentrations of the drug might inhibit the translation of the Erm cistron and delay the expression of resistance (Gaynor & Mankin, 2005).

Azithromycin is a macrolide antibiotic extensively used for treating respiratory tract infections, skin-related infections, and infections attributable to Gram-positive bacteria. Exceptionally, azithromycin has also exhibited high clinical efficacy against infections caused by *Salmonella*, which is a genus of Gram-negative bacteria. The use of azithromycin against *Salmonella* has proven to be effective in animal infection models, clinical trials, and clinical practice. Meanwhile, when tested *in vitro,* azithromycin is relatively ineffective against this pathogen as the minimum inhibitory concentration (MIC) of azithromycin exceeds the maximal concentration achievable in plasma (Matzneller et al., 2013).

1.3 Drug influx and efflux in Gram-negative bacteria

Bacteria are capable of developing resistance to antibiotics through various mechanisms, including alteration of cellular permeability to prevent the entry of the drug into the cells and pumping the drug out from the cellular milieu using efflux pumps. Gram-negative bacteria are intrinsically resistant to many antibiotics, thus, much harder to treat when compared to Gram-positive bacteria. The notorious resistance of Gram-negative bacteria is attributable to their unique cell envelope consisting of an outer membrane (OM) composed of lipopolysaccharides in its outer layer, and an inner membrane (IM) made up of a phospholipid bilayer. Between the two membranes lies the periplasm, which contains the peptidoglycan layer. The

OM typically impedes lipophilic molecules, whereas the IM imposes a barrier for hydrophilic solutes. Consequently, the OM in Gram-negative bacteria can serve as a frontline defence system against antibiotics by drastically decreasing the permeability of the drugs (Prajapati et al., 2021).

An antimicrobial drug needs to reach its requisite target site in the bacterial cell in order to be efficient. Thus, successfully crossing this envelope, particularly the outer membrane, is necessary for an effective antimicrobial treatment. Most Gram-negative bacteria accommodate nonspecific uptake protein channels (or porins) in their outer membrane (**Figure 4**). Porins mediate the transport or influx of small hydrophilic molecules (including antibiotics and nutrients) across the outer membrane and hence, are considered to be the main factors regulating drug permeability (Masi et al., 2017).

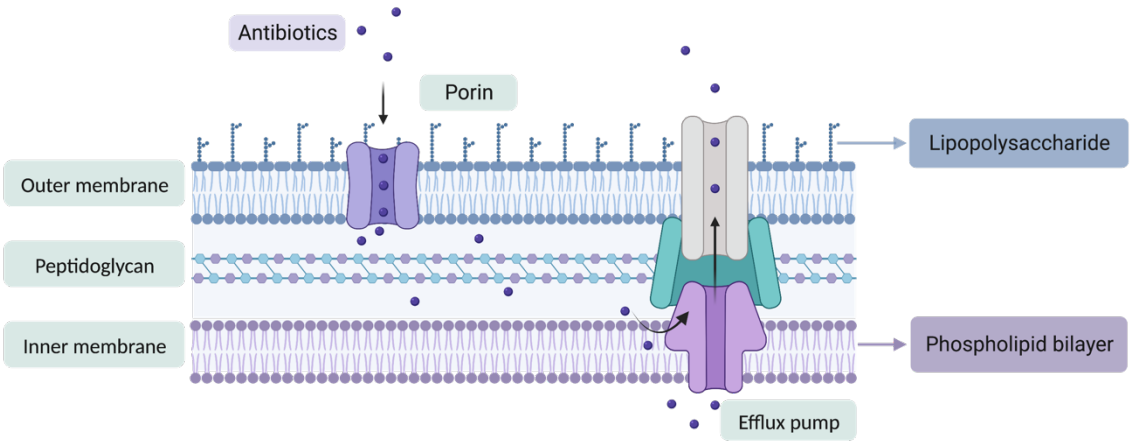

Figure 4. Schematic representation of the Gram-negative bacterial cell envelope. The bacterial cell envelope comprises an outer membrane, a thin peptidoglycan layer, and an inner membrane. This structure renders these bacteria resistant to numerous antibiotics. In addition, several pumps and channels are present in the cell envelope which are responsible for the influx of drugs (porins) or efflux of drugs out of the cellular milieu (efflux pumps). Figure adapted from Prajapati, Kleinekathöfer and Winterhalter, 2021.

In addition to the permeability barrier imposed by the outer membrane, drug efflux also plays a key role in the challenges of antibiotic treatment. Antibiotic efflux is the mechanism by which bacteria pump out the antibiotic from their cellular interior to the extracellular space through specific transporter proteins called efflux pumps. The efflux pumps transport substrates against a concentration gradient; thus, they are energy dependent. The energy is either

sourced from active hydrolysis of ATP, or chemical gradients formed by protons or ions. Furthermore, efflux pumps can be specific and extrude only a single class of antibiotics or able to pump out various classes of antibiotics. Considering the profound role of efflux in mediating antibiotic resistance, it is worthwhile to believe that abolishing efflux could enhance the activity of antibiotics on bacterial cells. There are several paths that lead to the inhibition of efflux pumps. Namely: 1) downregulating of efflux pump genes' expression, 2) redesigning antibiotics that are no longer recognized by the efflux pumps, 3) impeding the assembly of functional pumps, 4) blocking the pump to keep the substrate from binding to it, and 5) collapsing the energy mechanism in charge of providing the required energy for the action of the pumps (Ashima K. Bhardwaj & Priyabrata Mohanty, 2012). Efflux pump inhibitors (EPIs) are molecules that impede efflux pumps through one or more mechanisms and thereby inactivate antibiotic transport. The EPIs can be used in combination with antibiotics to potentiate their activity against bacteria expressing efflux pumps. Phenylalanyl arginyl β-naphthylamide (PAβN) was the first EPI to be discovered. While EPIs have the potential to give rise to a breakthrough in antimicrobial therapy, their success has been limited to *in vitro* studies and no EPI has made it to the commercial realm thus far (Sharma et al., 2019).

Furthermore, the susceptibility of Gram-negative bacteria to antibiotics can be escalated by increasing the permeability of the outer membrane toward antimicrobial drugs. Polymyxin B nonapeptide (PMBN) is a non-bactericidal cationic cyclic peptide that is derived by enzymatic processing of the naturally occurring polymyxin B (Tsubery et al., 2000). PMBN is capable of rendering the outer membrane of certain Gram-negative bacteria, such as *Salmonella enterica* and *E. coli* more permeable towards hydrophobic antibiotics. The activity of PMBN presumably relies on direct binding to the bacterial lipopolysaccharides (Vaara & Viljanen, 1985). It has been shown that PMBN raises the permeability of the outer membrane in a concentration-dependent manner and reduces the MIC when coupled with a macrolide such as Azithromycin, indicating the success of the combination in increasing the efficiency of treatment and lowering the required antimicrobial drug dose (Al-Marzooq et al., 2022a).

1.4 Persistent bacterial infections

Antibiotic resistance attained through genetic adaptation or horizontal gene transfer may facilitate the survival and growth of bacteria in the presence of antibiotics, even at high concentrations (Fisher et al., 2017). Additionally, treating bacterial infections caused by non-

resistant bacteria with appropriate antibiotics can result in a swift decrease in bacterial burden, but often fails to eliminate a fraction of bacterial cells that can cause relapses and chronic infections (Balaban et al., 2013). Plenty of bacterial infections can linger the host for extended periods, avoiding clearance by the host immune response or prolonged antibiotic treatment. A bacterial infection typically arises the host innate and adaptive immune response, which is usually sufficient to eliminate the infection. However, many pathogens have evolved survival mechanisms to evade the host immune response and thereby establish a persistent infection. Among the most predominant persistent infections are Typhoid fever, Urinary tract infection (UTI), tuberculosis, chronic wound infections, and Cystic fibrosis-related lung infections (Gollan et al., 2019). Persistent infections are typically distinguished by a long period of clinical manifestation, despite antimicrobial treatment. Various factors in both the pathogen and host contribute to the emergence of persistent infections. In the absence of antibiotic treatment, a persistent infection can arise from the failure of the host immune system to eradicate the pathogen. This may be a consequence of the immune system's inability to detect the pathogen. Certain bacteria, such as *Borrelia* spp., have developed strategies to prevent detection by the host (Norris, 2006). Moreover, pathogens can modulate host immune responses to provoke an inappropriate response which decreases the chance of pathogen clearance. In the presence of antibiotic treatment, persistent infections can occur due to several factors, such as poor pharmacokinetics of drugs in infected tissues (Gonçalves-Pereira & Póvoa, 2011).

Urinary tract infection (UTI) is a perfect example of bacteria hiding from the immune system and remaining obstinate to treatment, resulting in long courses of antibiotic treatment required to cure the infection. Uropathogenic *Escherichia coli* (UPEC) is a common cause of recurring urinary tract infections. Studies suggest that following a urinary tract infection caused by uropathogenic *Escherichia coli*, 20% to 30% of women suffer from the reappearance of symptoms. Such reappearance of an infection may in fact be a consequence of either relapse or reinfection. Relapse is when the symptoms of the initial infection temporarily diminish until the reservoir of bacteria that was not cleared out in the first infection episode gets reactivated. Reinfection, on the other hand, appears when a new contamination occurs after complete clearance of the initial infection (Gollan et al., 2019). Typhoid fever is another prevalent bacterial infection caused by the Gram-negative intracellular bacterium, *Salmonella enterica* subspecies *enterica* serovar Typhimurium (*S.* Typhi). Statistics indicate that Typhoid fever tends to recur in 15% of patients following antimicrobial therapy (Gotuzzo et al., 1987).

1.5 Intracellular infections

Intracellular infections are maladies caused by intracellular bacteria, which are pathogens that must enter host cells to reproduce. These pathogens rely on survival and replication inside the host cell to be able to proliferate and lead to an infectious disease. Within the host cell, they can evade cellular defence mechanisms and remain secured from detection and elimination by the humoral defence system and antimicrobials. Typically, some intracellular pathogens proliferate in the host cell's cytosol, while others replicate within membrane-bound vacuoles or phagosomes. For instance, the majority of *S.* Typhimurium replicate inside *Salmonella*-containing vacuoles (SCVs) upon invading epithelial cells. Nonetheless, numerous species are also capable of residing at more than one cellular compartment (Helaine & Holden, 2013).

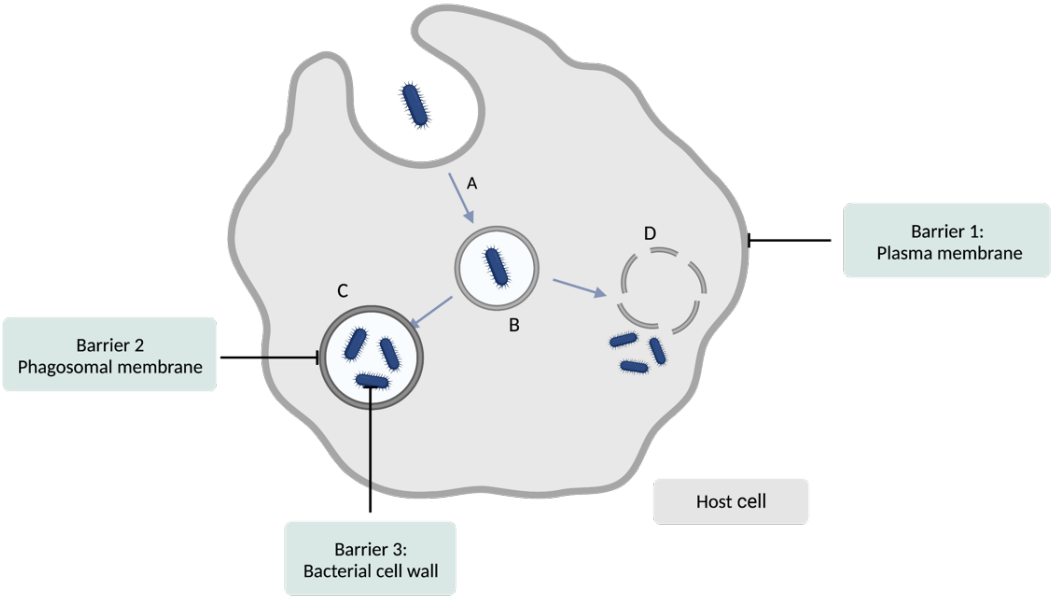

Figure 5. Localization of bacteria inside the host cell and the barriers to antibiotics. Upon entry to the host cell (**A**), bacteria are typically enclosed inside endosomes (**B**). They can survive and proliferate within endosomes as they mature into phagosomes (**C**). Additionally, certain bacteria can induce endosome rupture and thereby enter the cytosol (**D**). The black arrows signify three significant barriers that antimicrobials face to reach intracellular bacteria: 1) the plasma membrane of the host cell, 2) the phagosomal membrane, 3) the bacterial cell wall. Figure adapted from Kamaruzzaman, Kendall and Good, 2017.

Intracellular infections are challenging to treat as the antimicrobial drug must cross many barriers to reach its target pathogen (**Figure 5**). First and foremost, the antibiotic should get

through the plasma membrane (Kamaruzzaman et al., 2017). The plasma membrane of mammalian cells comprises a lipid bilayer including peripheral and integral proteins and is impermeable to most polar or charged solutes. While certain antimicrobial groups such as macrolides and quinolones have the capability to diffuse across the lipid bilayer, they still face the threat of being depleted by efflux pumps (Tulkens, 1991). Upon entering the host cell, the antimicrobials should accumulate at sufficient concentrations for an adequate period in order to be efficient. Thus, the action of efflux pumps can be very critical in the treatment efficacy as they can prevent the drug from reaching the desired intracellular concentration, thereby keeping them from reaching the pathogen. After successfully accumulating inside the host cell, the antibiotics face the second barrier, reaching the compartment in which the bacteria reside (Kamaruzzaman et al., 2017). The specific intracellular location of bacteria (vacuole, cytosol, or phagosome) can propose additional challenges to antimicrobial treatment. Namely, *Salmonella* often localizes in acidified vacuoles where the pH can drop to 4.0-5.0, and the respective antibacterial should resist acidic pH to lead to successful treatment (Rathman et al., 1996). Lastly, the antimicrobial drug should cross the bacterial cell wall to reach its specific target within the bacterial cell. In case of infections caused by Gram-negative bacteria, this step proposes additional challenges to the treatment due to the difficulty of crossing the outer membrane of these bacteria, as mentioned previously (Prajapati et al., 2021).

1.6 Fluorescent bioreporters

Fluorescent bioreporters are genetically encoded reporters of intracellular processes, signalling pathways, or biomolecule concentrations, whose output can be quantified through fluorescence microscopy or spectrometry (Aktar et al., 2022). Most bioreporters are products of genetic engineering, by which a promoter that is responsive to a stimulus is fused with a reporter gene that encodes a fluorescent product (Leveau & Lindow, 2002). Bioreporters can be used to detect physical signals such as ultraviolet radiation (Kim & Sundin, 2000) as well as chemical substances such as nutrients (Miller et al., 2001), antibiotics (Hansen et al., 2001), and metals (Joyner & Lindow, 2000). Additionally, fluorescent reporter genes are frequently used to shed light on gene expression or the activity of a promoter. For this purpose, a reporter gene can be placed downstream the gene or promoter of interest to indicate the expression of the gene or induction of the promoter, as depicted in **Figure 6** (Chalfie et

al., 1994). Green fluorescent protein (GFP) is amidst the most predominantly utilized reporters in both prokaryotic and eukaryotic cells due to its highly specific output with high signal-to-noise ratios (Cambré & Aertsen, 2020).

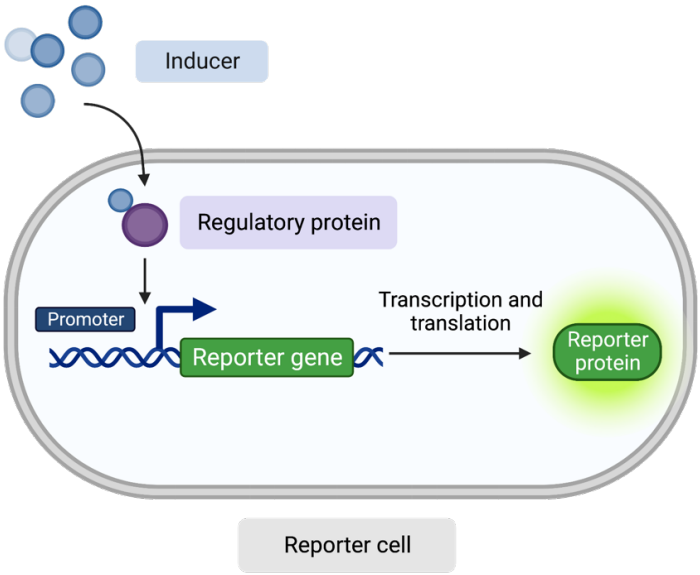

Figure 6. General schematic of an inducible intracellular fluorescent bioreporter. The reporter gene is located downstream of an inducible promoter. In the presence of the inducer molecule, the promoter is positively regulated, and the reporter gene is expressed. Figure adapted from (Zhu et al., 2022).

Furthermore, the dilution of a pre-synthesized fluorescent protein can be employed to observe bacterial cell division. In growing cells, the amount of the pre-synthesized fluorescent protein decreases with each cell division, whereas in non-growing cells, the fluorescent protein maintains a constant amount. Therefore, monitoring the fluorescence signal intensity over time enables individual cell divisions to be tracked and different subpopulations to be distinguished in the growing bacterial culture (Roostalu et al., 2008).

2 THE AIMS OF THE THESIS

In this work we aimed to:

- test the efficiency of azithromycin against uropathogenic *E. coli* CFT073 in standard conditions and conditions that resemble the infection sites.
- validate the use of fluorescent reporters in detecting the exposure of bacteria to macrolide antibiotics.

3 EXPERIMENTAL PART

3.1 MATERIALS AND METHODS

3.1.1 Bacterial strains

a) *E. coli* CFT073

b) *E. coli* DH5α

3.1.2 Plasmids

The plasmids used in this study are listed in **Table 1**.

Table 1. Plasmids used in this study. Each row in the table contains the name of the plasmid, the plasmid's content, the antibiotic resistance marker, and the source.

Plasmid	Description	Resistance marker	Source
pZb-ErmCL-GFP	pTrc promoter, ErmCL leader peptide, GFP reporter	AMP	Mankin lab
pZb- ErmCL-KAT	pTrc promoter, ErmCL leader peptide, KAT reporter (Shcherbo et al., 2007)	AMP	Mankin lab
pZb-ErmCL-RFP	pTrc promoter, ErmCL leader peptide, RFP reporter	AMP	Mankin lab
pZb-ErmALCL-RFP	pTrc promoter, ErmAL leader peptide, ErmCL leader peptide, RFP reporter	AMP	Mankin lab
pBAD33	araBAD promoter, *araC* regulatory gene	CHL	(Guzman et al., 1995)
pSC101-GFP-Pcda-iSc	cda promoter, mScarlet reporter	AMP	Tenson lab
pSC101-Timer-TetR-TetA-BFP-noDeg	10.CE promoter, tetR repressor, BFP reporter	KAN	Tenson lab
pBAD33-mScarlet	araBAD promoter, *araC* regulatory gene, mScarlet reporter	CHL	This Study
pSC101-ErmCL-GFP-mScarlet	10.CE promoter, ErmCL leader peptide, GFP reporter, mScarlet reporter	KAN	This Study

3.1.3 Growth media and buffers

The following media were used for bacterial growth.

a) Super Optimal Broth (SOB): 28 g of BD Difco™ SOB Medium powder (Product number 244310) containing 20 g/l tryptone, 5 g/l yeast extract, 0.5 g/l sodium chloride, 2.4 g/l magnesium sulfate, and 0.186 g/l potassium chloride, dissolved in purified water and autoclaved. Final pH 7.0 ± 0.2.
b) Super Optimal Broth with Catabolite repression (SOC): SOB supplemented with 0.2% Glucose.
c) Luria-Bertani (LB) broth: 20 g of BD Difco™ LB broth powder (Product number 240230) containing 10 g/l tryptone, 5 g/l yeast extract and 5 g/l NaCl, dissolved in purified water and autoclaved. Final pH 7.0 ± 0.2.
d) Cation-adjusted Mueller-Hinton Broth (Ca-MHB): 22 g of BBL™ Ca-MHB powder containing 3 g/l beef extract, 17.5 g/l acid hydrolysate of casein, and 1.5 g/l starch, dissolved in deionized water and autoclaved. 40 mM HEPES buffer pH 7.4 was added after autoclaving.
e) Low phosphate, low magnesium-containing medium (LPM): 5 mM Potassium chloride, 7.5 mM Ammonium sulfate, 0.5 mM Potassium sulfate, 0.337 mM Sodium phosphate monobasic monohydrate dissolved in deionized water and autoclaved. 0.3% Glycerol, 0.1% Casamino acids, 49 µM $MgCl_2$ and 30 mM MES buffer pH 5.5 or 40 mM HEPES buffer pH 7.4 was added after autoclaving (Coombes et al., 2004).
f) Dulbecco's Modified Eagle's Medium (DMEM): ATCC® 30-2002. 40 mM HEPES buffer pH 7.4 was added.
g) Rosewell Park Memorial Institute Medium (RPMI-1640) supplemented with HEPES: Thermo Fisher Scientific Gibco™ catalog number 22400089.

The following buffers were used for the growth media:

a) HEPES buffer: 0.4 M HEPES buffer was prepared by dissolving the FisherBioreagnets™ HEPES powder (Catalog number BP310-100) in distilled water. The pH was adjusted to 7.4 using 10 M KOH solution. The buffer was then filtrated using 0.22 µm pore filter and stored at -20°C.
b) MES buffer: 0.3 M MES buffer was prepared by dissolving the AppliChem MES anhydrous powder (Product code A0689) in distilled water. The pH was adjusted to 5.5 using 5 M KOH solution. The buffer was then filtrated using 0.22 µm pore filter and stored at -20°C.

3.1.4 Antibiotic solutions

Several antibiotic solutions were used in this study, as displayed in **Table 2**. All antibiotic solutions were stored at -20°C.

Table 2 Antibiotic stock solutions used in this study. Each row in the table contains the antibiotic's name, the concentration of the stock solution, the respective solvent, and manufacturer.

Antibiotic	Concentration	Solvent	Manufacturer, product number
Ampicillin	100 mg/ml	H_2O	Fisher Bioreagents™, BP1760-25
Azithromycin	32 mg/ml	96% Ethanol	Carbosynth limited, AD296571701
Clarithromycin	32 mg/ml	96% Ethanol	Carbosynth limited, AC204691501
Chloramphenicol	5 mg/ml	96% Ethanol	AppliChem, A1806
Erythromycin	32 mg/ml	96% Ethanol	Sigma Aldrich, E0774
Josamycin	32 mg/ml	96% Ethanol	Cayman Chemical, CAYM29606
Kanamycin	25 mg/ml	H_2O	AppliChem, A1493
Midecamycin	10 mM	DMSO	MedChemExpress, HY-B1908
Oleandomycin	25 mg/ml	96% Ethanol	Sigma Aldrich, T6514
Rosamicin	2.5 mM	DMSO	Vitas-M Chemical Limited, STK256720
Solithromycin	10 mM	DMSO	Cayman Chemical, CAYM21681
Telithromycin	10 mM	DMSO	Sigma Aldrich, SML2162
Tylosin	10 mM	DMSO	European Pharmacopeia Reference Standard, T2880000

3.1.5 Competent cell preparation

A single *E. coli* CFT073 colony was inoculated in 3 ml of LB and incubated overnight at 37°C, 200 rpm. 0.4 ml of the overnight culture was diluted in 40 ml of SOB broth in a 250 ml flask and incubated at 37°C, 200 rpm till the optical density at 600 nm reached 0.4 (mid

exponential growth phase). The culture was transferred to a 50 ml Falcon tube and incubated on ice for 15 minutes. Consecutively, the culture was centrifuged at 5000 G for 15 minutes at 4°C. The supernatant was removed, and the pellet was resuspended in a 2 ml RF1 buffer containing 100 mM RbCl, 50 mM $MnCl_2$, 30 mM Potassium acetate, 10 mM $CaCl_2$, 15% Glycerol (pH 5.8). The cells were kept on ice for 15 minutes and another round of centrifugation was performed in the same conditions. The supernatant was removed, and the pellet was resuspended in 2 ml RF2 buffer containing 10 mM MOPS (pH 6.8), 10 mM RbCl, 75 mM $CaCl_2$, 15% Glycerol. The competent cells were aliquoted into 1.5 ml Eppendorf tubes, with each containing 100 µl, frozen in liquid nitrogen, and stored at -80°C.

3.1.6 Bacterial transformation

E. coli competent cells were taken from -80°C and thawed on ice. DNA was added to 100 µl of the competent cells, mixed, and consecutively incubated for 30 minutes. The mixture was then heat-shocked for 2 minutes at 42°C, followed by cooling down on ice. Subsequently, 1 ml of SOC medium was added to the mixture and incubated for 60 minutes at 37°C. The cells were plated out on LB agar plate containing the selective antibiotic and incubated overnight at 37°C.

3.1.7 Plasmid extraction

A colony taken from an LB agar plate was inoculated in 3 ml LB medium containing the corresponding antibiotic. The glass tube was then incubated at 37°C, 200 rpm overnight. Plasmid DNA was isolated from the bacterial cells using the FavorPrep Plasmid Extraction Mini Kit (Favorgen) according to the manufacturer's protocol. The concentration of the purified DNA was assessed by Thermo Fisher's NanoDrop 1000 Spectrophotometer.

3.1.8 Minimum Inhibitory Concentration (MIC) determination

A single *E. coli* CFT073 colony was inoculated into 3 ml LB and grown overnight at 37°C, 200 rpm. The overnight culture was diluted 100x in 30 ml LB and incubated at 37°C, 200 rpm for 60 minutes. In the meantime, dilutions of the of antibiotics were prepared in the testing medium. 200 µl of the testing medium bearing antibiotic was loaded on wells 1-10 of row A of the 96-well microtiter plate, and 100 µl of the testing medium without any antibiotics was loaded in all the remaining wells of columns 1-10. Subsequently, 2x serial dilutions were made in the range A to H. 200 µl of testing medium without any antibiotics was loaded in wells 11 and 12 of row A for the positive and negative control, respectively. The resuscitated culture was further diluted 100x in 20 ml of the testing medium. Consecutively,

100 µl of the diluted culture was added to all the wells in columns 1-11 and 100 µl of the medium to every well in column 12. The plate was incubated at 37°C overnight, and the MIC was determined by visually analyzing the plate. The lowest concentration in which no growth was visible accounts for the minimum inhibitory concentration of the tested antibiotic in given conditions.

3.1.9 Measurement of reporter gene expression on 96-well microtiter plate

The transformed *E. coli* CFT073 colony bearing a reporter plasmid was inoculated in 3 ml LB supplemented with the corresponding selective antibiotic and grown overnight at 37°C, 200 rpm. On the following day, the overnight culture was diluted 100x in 20 ml of buffered testing medium (Ca-MHB or LPM). Subsequently, the diluted culture was grown at 37°C, 200 rpm, until the optical density at 600 nm was approximately 0.2. Once the desired optical density was reached, 1 mM of IPTG (isopropylthio-β-D-1-galactoside) was added to the culture to induce transcription, followed by 30 minutes of incubation at 37°C and 200 rpm. Meanwhile, 1 ml of buffered testing medium (Ca-MHB or LPM) containing 1 mM IPTG and corresponding macrolides was prepared. 200 µl of the antibiotic-containing medium was added to the wells of row B. 100 µl of the testing medium was loaded in all the other wells of the microtiter plate, followed by 2x serial dilutions in the range B to H. 100 µl of the *E. Coli* CFT073 culture was added to every well on the plate. Subsequently, the plate was placed in the BioTek Synergy H1 microplate reader to measure the optical density at 600 nm (OD_{600}) and fluorescence of the fluorophores in 10-minutes intervals during a time span of 12 hours in 37°C. The excitation and emission wavelength range of each fluorescent protein is listed in **Table 3**.

Table 3. Excitation and emission wavelengths used in the microplate reader for detection of the fluorescent proteins.

Fluorescent protein	Excitation range (nm)	Emission range (nm)
Green Fluorescent Protein (GFP)	485 ± 5	510 ± 5
Katushka (KAT)	588 ± 5	635 ± 25
Red Fluorescent Protein (RFP)	583 ± 10	630 ± 10
mScarlet	569 ± 10	594 ± 10

3.1.10 Measurement of reporter gene expression by flow cytometry

The bacterial cultures were grown in HEPES-buffered Ca-MHB (pH 7.4), diluted, and supplemented with azithromycin and 0.2% L-arabinose (if needed) following the same procedure that was used to measure the expression of reporters in the 96-well microtiter plates. The plate was wrapped in parafilm and incubated at 37°C. 20 µl aliquots were taken and mixed with an equal volume of sterile 30% glycerol at three different time points: prior to incubation, after 2 hours of incubation, and after 4 hours of incubation. The samples were frozen in liquid nitrogen upon collection and stored at -80°C. The samples were thawed on ice, and the concentration of the bacteria was adjusted to approximately 10^6 CFU/ml by addition of Phosphate-buffered saline (PBS). If needed, the cells were stained with 1 µl of FM™ 4-64 dye (Thermo Fisher Scientific catalog number T13320) to distinguish bacteria from the noise by staining the bacterial cell membrane. The samples were analyzed using Attune NxT Flow Cytometer.

3.1.11 Plasmid design and PCR

Two plasmids pSc101-ErmCL-GFP-mScarlet and pBAD33-mScarlet were designed. The former was constructed so that the leader peptide encoding sequence, GFP, and mScarlet would be placed downstream 10.CE constitutive promoter. The latter was constructed to insert mScarlet under the control of the araBAD promoter, regulated by L-arabinose. The fragments obtained from each template plasmid and the respective primers are indicated in **Table 4.** The 5'-3' sequences of primers used are depicted in **Table 5.** For cloning of the 696 bp mScarlet fragment, plasmid pBAD33 was digested using FastDigest™ restriction enzymes HindIII (Thermo Fisher Scientific catalog number FD0504) and SacI (Thermo Fisher Scientific catalog number FD1133). The digestion was carried out at 37°C for 15 minutes. The restrictase digestion reaction mixture is shown in **Table 6**. Polymerase chain reaction was performed using Thermo Scientific Phusion High-Fidelity DNA Polymerase (Thermo Fisher Scientific catalog number F530L). The PCR reaction mix's final volume was 50 µl, and the exact components are presented in **Table 7**. The PCR program used for the amplification of the DNA fragments is shown in **Table 8**. Annealing temperature and DNA extension times were estimated separately for every set of primers**.** 50 µl of the PCR products and restricted pBAD33 were mixed with 10 µl of 6x Orange DNA Loading Dye (Thermo Fisher Scientific catalog number R0631) and loaded on 1% agarose gel containing Atlas ClearSight DNA Stain (Bioatlas catalog number BH40501). Electrophoresis was performed at 100 V. DNA gel electrophoresis was performed in 1x TAE (Tris-acetate-EDTA) buffer

with GeneRuler 1 kb DNA ladder (Thermo Fisher Scientific catalog number SM0311) as a size marker. DNA bands of the correct size were cut out from the agarose gel under UV light. The DNA was extracted with ZymoClean™ Gel DNA Recovery kit according to the manufacturer's protocol.

Table 4. Plasmid fragments to be amplified and corresponding primers.

Fragment to be amplified	Template plasmid	Primer 1	Primer 2	Fragment size
ErmCl + GFP	pZb-ErmCL-GFP	Up_ErmCl	Dwn_GFP	961 bp
Vector	pSC101-Timer-TetR-TetA-BFP-no-Deg	Vector_top	Vector_dwn	3605 bp
mScarlet	pSC101-GFP-Pcda-iSc	mScarlet_up	mScarlet_dwn	775 bp
mScarlet	pSC101-GFP-Pcda-iSc	mScarlet_For-ward	mScarlet_Re-verse	696 bp

Table 5. Primers used in this study. Each row in the table depicts the primers name and its 5'-3' sequence.

Name	**5'→3' sequence**
vector_top	TAGAGGATCCTCTATCAGCTCATTGAGCT
vector_dwn	AAGCAGCATAACCTTTTTCCGTGAT
up_ErmCl	AGCTCAATGAGCTGATAGAGGATCCTCTAATGTGTGGAATTGTGAGCGGATAAC
dwn_GFP	CGGGCTAGAGAATTCTTATTTTTCGAACTGC
mScarlet_dwn	ATCACGGAAAAAGGTTATGCTGCTTTTAGGCGGTCACTTGTACAGCTCG
mScarlet_up	CGCAGTTCGAAAAATAAGAATTCTCTAGCCCGGGAGGTGCAATATGGTGAGCAAG
mScarlet_Forward	TTGGGCTAGCGAATTCGAGCTGAGGTGCAATATGGTGAGCAAG
mScarlet_Reverse	CGCCAAAACAGCCAAGCTTTAGGCGGTCACTTGTACAGCTCG

Table 6. Restriction reaction mixture.

Component	µl	Final concentration
pBAD33 (40 ng/µl)	15	30 ng/µl
Nuclease-free water	2	-
FastDigest™ Buffer (10x)	2	1x
FastDigest™ HindIII	0.5	-
FastDigest™ SacI	0.5	-

Table 7. PCR mixture.

Component	µl	Final concentration
DNA Template	1.5	0.2-2 ng/µl
5x Phusion PCR Buffer (Thermo Fisher Scientific)	10	1x
dNTPs (10 mM)	1	0.2 mM
Phusion High Fidelity DNA Polymerase (Thermo Fisher Scientific) (2 U/µl)	0.5	1 U
Primer 1	2	4 µM
Primer 2	2	4 µM
Nuclease-free water	33	-

Table 8. PCR program.

Cycle step	Temperature (°C)	Time (s or min)	Number of Cycles
Initial Denaturation	98	3 min	1
Denaturation	98	10 s	32
Annealing	60	30 s	
Extension	72	1 min	
Final extension	72	5 min	1

3.1.12 Circular Polymerase Extension Cloning (CPEC)

The plasmids were constructed by the CPEC method, which is based on polymerase overlap extension and joins overlapping DNA fragments into a double-stranded circular form (Quan & Tian, 2009). The plasmid pBAD33-mScarlet was assembled from the pBAD33 vector fragment and 696 bp mScarlet insert. The plasmid pSC101-ErmCL-GFP-mScarlet was assembled from pSC101-Timer-TetR-TetA-BFP-noDeg vector fragment and GFP reporter with the preceding ErmCL leader peptide encoding sequence, and 775 bp mScarlet inserts. The final volume of the CPEC reaction mixture is 20 µl, and the exact components of the mixture are listed in **Table 9**. The CPEC program used for assembling the fragments is shown in **Table 10**. The CPEC reaction mixture was transformed into DH5α competent cells. The plasmid was purified from the transformants and transformed into CFT073 competent cells.

Table 9. CPEC reaction mixture.

Component	µl	Final concentration
Vector Fragment	2.5	Insert and vector molar ratio of 1:1
Insert Fragment(s) (GFP and/or mScarlet)	11	
5x Phusion HF Buffer (Thermo Fisher Scientific)	4	1x
dNTPs (10 mM)	2	1 mM
Phusion High Fidelity DNA Polymerase (Thermo Fisher Scientific) (2 U/µl)	0.5	1 U/µl

Table 10. CPEC reaction program.

Cycle step	Temperature (°C)	Time (s or min)	Number of Cycles
Initial Denaturation	98	45 s	1
Denaturation	98	15 s	25
Annealing	From 70 to 55	30 s	
Extension	72	5 min 30 sec	
Final extension	72	10 min	1

3.1.13 Testing reporter gene expression on solid medium

A single *E. coli* CFT073 colony bearing pZb-ErmCL-GFP or pZb-ErmCL-KAT reporter plasmid was inoculated in 3 ml LB medium supplemented with 100 μg/ml ampicillin and grown overnight at 37°C, 200 rpm. Two variations of agar plates were prepared using MOPS and LPM media. The exact composition of the plates is depicted in **Table 11 and 12**.

Table 11. MOPS agar plate composition.

Component	Amount (ml)	Final concentration
3% Autoclaved BD Bacto™ Agar in H_2O	100	1.5%
Autoclaved distilled H_2O	76	-
10x MOPS (Neidhardt et al., 1974)	20	1x
20% Sterile glucose	2	0.2%
132 mM K_2HPO_4	2	1.32 mM

Table 12. LPM agar plate composition.

Component	Amount (ml)	Final concentration
3% Autoclaved BD Bacto™ Agar in H_2O	100	1.5%
Autoclaved distilled H_2O	55.9	-
10x LPM	20	1x
10% Casamino acids	2	0.1%
30% Glycerol	2	0.3%
1 M $MgCl_2$	0.0098	49 μM
0.4 M HEPES buffer (pH 7.4)	20	40 mM

80 µl of 1 M IPTG was spread on the plates to induce the transcription of the reporter gene. The plates were left to dry for approximately 30 minutes. 80 µl of the overnight culture was spread on the plate evenly. Filter discs were placed on the plate and 2 µl of testing antibiotic was added to each disc. All antibiotics were diluted in Milli-Q water. The plates were incubated overnight at 37°C and analyzed using the Amersham™ Typhoon™ Biomolecular Imager. Katushka fluorescence was scanned using 532 nm laser and Cy5 filter, the central wavelength of which is 670 nm with a bandwidth of 30 nm. GFP fluorescence was scanned using 488 nm laser and Cy2 filter, the central wavelength of which is 525 nm with a bandwidth of 20 nm.

3.2 RESULTS AND DISCUSSION

3.2.1 MIC of macrolide antibiotics is affected by pH and composition of the growth media

Macrolides such as azithromycin are often clinically used in order to treat infections caused by Gram-positive bacteria. Exceptionally, azithromycin has displayed high clinical efficacy in treating infections caused by *Salmonella*, which is a Gram-negative bacterium. Studies report that the maximum achievable plasma concentration for Azithromycin (0.5 μg/ml) is noticeably lower than the published MIC values, which are in the 4-8 μg/ml range (Matznel-ler et al., 2013). Therefore, the mechanism underlying the efficacy of azithromycin against Gram-negative bacteria such as *Salmonella* remains enigmatic. In this work, we aimed to decipher the mechanisms of macrolide activity against another Gram-negative bacterium, uropathogenic *Escherichia coli* CFT073.

First and foremost, the minimum inhibitory concentration (MIC) was measured in various growth media to note how sensitivity to macrolides is affected by conditions that can differ between the standard testing medium and infection sites. The MIC of three macrolide anti-biotics, azithromycin, clarithromycin, and erythromycin was determined in HEPES-buffered Ca-MHB (pH 7.4), which is the standard medium for testing antimicrobial activity, and MES-buffered LPM (pH 5.5) which mimics the conditions within acidified vacuoles or phagosomes. As depicted in **Table 13**, the MIC values of all three macrolides were notice-ably lower in HEPES-buffered Ca-MHB (pH 7.4) compared to MES-buffered LPM (pH 5.5). We suspected that this demonstrates the dependence of the activity of these macrolides on pH, and lower efficiency in acidic pH. Macrolides are protonated at an acidic pH, while they are capable of permeating through cytoplasmic membranes in their uncharged form only. Thus, their access to intracellular targets and accumulation in cells is reduced at an acidic pH, leading to elevated MICs (Dalhoff et al., 2005).

Table 13. The minimum inhibitory concentrations of azithromycin, clarithromycin, and erythromycin in different pH conditions.

	Azithromycin	Clarithromycin	Erythromycin
HEPES-buffered Ca-MHB (pH 7.4)	4 µg/ml	64 µg/ml	128 µg/ml
MES-buffered LPM (pH 5.5)	> 256 µg/ml	512 µg/ml	> 512 µg/ml

Therefore, we tested the susceptibility of UPEC to azithromycin in LPM at neutral pH and utilized other media with different ionic conditions that are similar to those found in infected tissues. LPM medium has low phosphate and magnesium content, which resemble the concentrations within a vacuole inside the infected host cells. Ca-MHB, on the other hand, is enriched with divalent cations: Ca^{2+} (20-25 mg/l) and Mg^{2+} (10-12.5 mg/l). These play a crucial role in stabilizing the lipopolysaccharide layer of the bacterial cell membrane, thereby reducing the permeability of the outer membrane (Murata et al., 2007). In addition, two cell-culture media, DMEM and RPMI, were tested.

Furthermore, the infected tissues contain antimicrobial peptides (Lin et al., 2015). Therefore, the MIC of Azithromycin was determined in the presence of 10 µg/ml PMBN (Polymyxin B Nonapeptide), which is a non-bactericidal peptide capable of increasing the permeability of the outer membrane of *E. coli* towards hydrophobic antibiotics. To test the role of azithromycin efflux, we also used 10 µg/ml PAβN, an efflux pump inhibitor that prevents the antimicrobial drug from being pumped out of the bacterial cell. In LPM and RPMI media, the MICs were 8-fold lower than in Ca-MHB and were indeed closer to the maximal plasma concentration of azithromycin. The addition of PMBN to the LPM medium further diminished the MIC of azithromycin to a level that is 50-fold lower than its maximal plasma concentration. A similar reduction pattern was observed upon addition of PAβN in all media. However, the combination of PMBN and PAβN did not lead to any additional decrease in LPM and DMEM media, while a 4-fold reduction was perceived in Ca-MHB and RPMI when both PMBN and PAβN were present. All in all, both PMBN and PAβN reduced the MIC (**Table 14**), thereby increasing the efficacy of treatment with a lower antimicrobial drug

dose. This result is also in agreement with previously published data demonstrating the synergistic effect of PMBN and azithromycin (Al-Marzooq et al., 2022).

Table 14. The effect of PMBN and PAβN on the minimum inhibitory concentration of azithromycin in four different media.

	Azithromycin	Azithromycin + PMBN	Azithromycin + PAβN	Azithromycin + PMBN + PAβN
HEPES-buffered Ca-MHB (pH 7.4)	4 µg/ml	0.5 µg/ml	0.25 µg/ml	< 0.0625 µg/ml
HEPES-buffered LPM (pH 7.4)	0.5 µg/ml	0.01 µg/ml	0.01 µg/ml	0.01 µg/ml
HEPES-buffered DMEM (pH 7.4)	2 µg/ml	1 µg/ml	1 µg/ml	1 µg/ml
HEPES-buffered RPMI (pH 7.2)	0.5 µg/ml	0.25 µg/ml	0.25 µg/ml	< 0.0625 µg/ml

The results indicate that if the conditions in the infection site resemble that of LPM and RPMI media, and the antimicrobial peptides present at the infection site enhance the effect of azithromycin in a similar manner to PMBN; then azithromycin is expected to work efficiently against UPEC as the MIC is in fact lower than the maximum concentration achievable in the plasma.

3.2.2 Fluorescent proteins can be used as reporters of macrolide exposure

Our aim was to build a fluorescent reporter that is induced explicitly in bacteria by macrolide antibiotics, foremost azithromycin. This would enable the possibility to observe whether bacteria encounter the drug in intracellular cell culture infection or animal infection model. Thereby, we would know if azithromycin can reach the infecting bacteria, when this happens, and if bacteria in different tissues and intracellular locations are evenly exposed to the drug. Four reporter plasmids were received from the Alexander Mankin lab: pZb-ErmCL-GFP, pZb-ErmCL-KAT, pZb-ErmCL-RFP, and pZb-ALCL-RFP. The plasmids contain a reporter gene (GFP, KAT, or RFP) which is preceded by the regulatory leader peptide coding sequence of the macrolide resistance gene, ErmCL (**Figure 7**). Exceptionally, pZb-ALCL-RFP bears two leader peptide encoding sequences upstream of the reporter gene, ErmAL

and ErmCL. The presence of the leader peptide open reading frame (ORF) renders the translation of the corresponding mRNA inducible by macrolides such as azithromycin. The reporter genes and their preceding leader peptide ORF are placed downstream of the pTrc inducible promoter, which contains lac operator and is hence regulated by lacI. The transcription of the reporter gene relies on the presence of IPTG (isopropylthio-b-D-1-galactoside), which binds to the repressor protein and prevents it from binding to the promoter, thus inducing the transcription of the reporter and its preceding leader peptide encoding sequence.

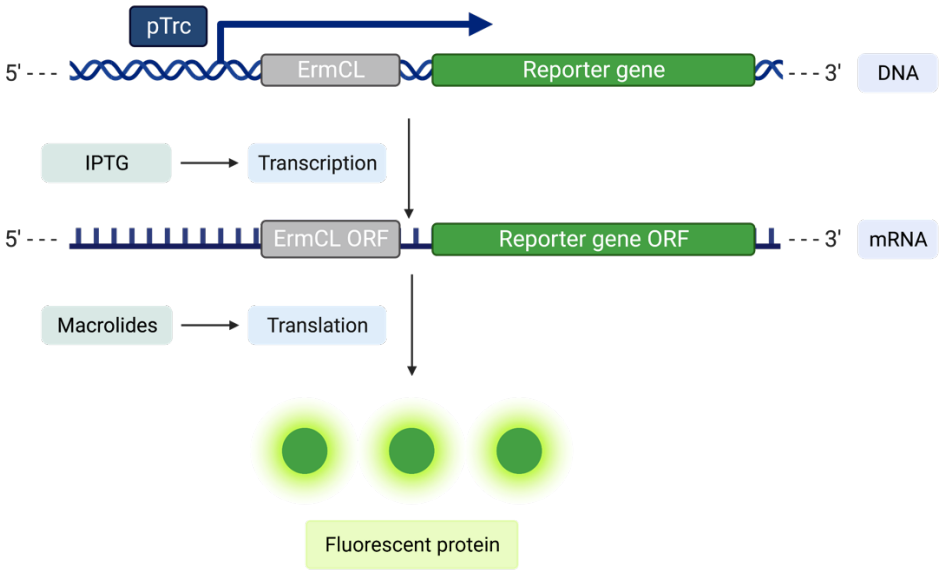

Figure 7. The working principle of the macrolide reporter plasmid. The transcription of the reporter gene is controlled by the pTrc promoter, which is induced by IPTG. The ErmCL leader peptide encoding sequence precedes the reporter gene ORF, making the translation of the reporter inducible by macrolide antibiotics. The successful translation of the reporter gene results in the production of reporter fluorescent proteins.

3.2.3 GFP and KAT-based reporter plasmids are capable of detecting macrolide antibiotics

Primarily, the expression of four reporter genes (GFP, KAT, RFP, ALCL-RFP) was assessed in the presence of azithromycin, clarithromycin, and erythromycin. The measurements were carried out in HEPES-buffered Ca-MHB (pH 7.4). RFP (**Figure 8**) and ALCL-RFP (**Figure 9**) exhibited very weak fluorescent signals in the presence of the macrolides of interest, with the lowest being the signal induced by azithromycin. The inadequate expression of RFP limits its competency to be used as an intracellular reporter *in vivo*. Consequently, RFP and ALCL-RFP were eliminated and not tested further.

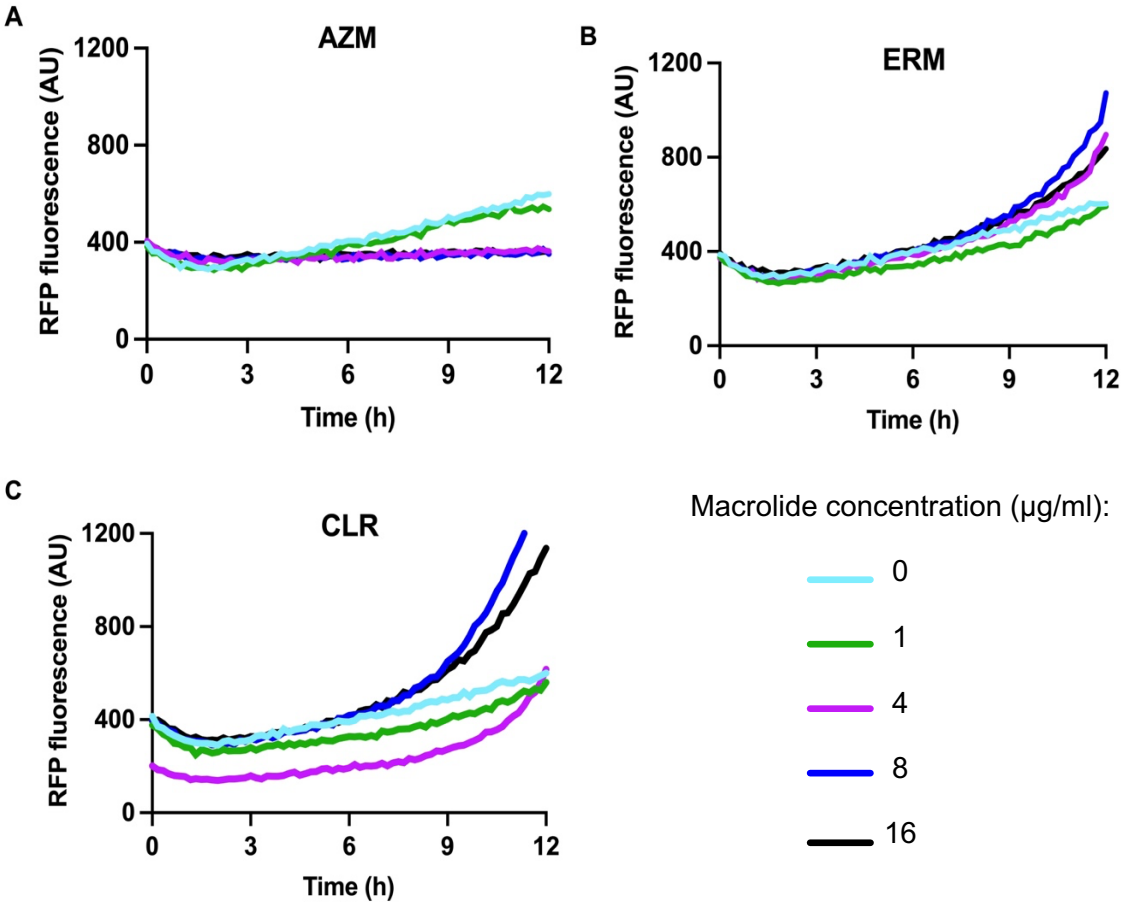

Figure 8. Induction of the RFP fluorescence in bacteria bearing pZb-ErmCL-RFP reporter plasmid by macrolides. The expression of the RFP reporter gene in pZb-ErmCL-RFP plasmid is induced with azithromycin (**A**), erythromycin (**B**), and clarithromycin (**C**) in Ca-MHB medium at pH 7.4. Fluorescence intensity was measured in 10-minute intervals within 12 hours using microplate reader. The Y-axis represents the intensity of the fluorescence in arbitrary units (AU).

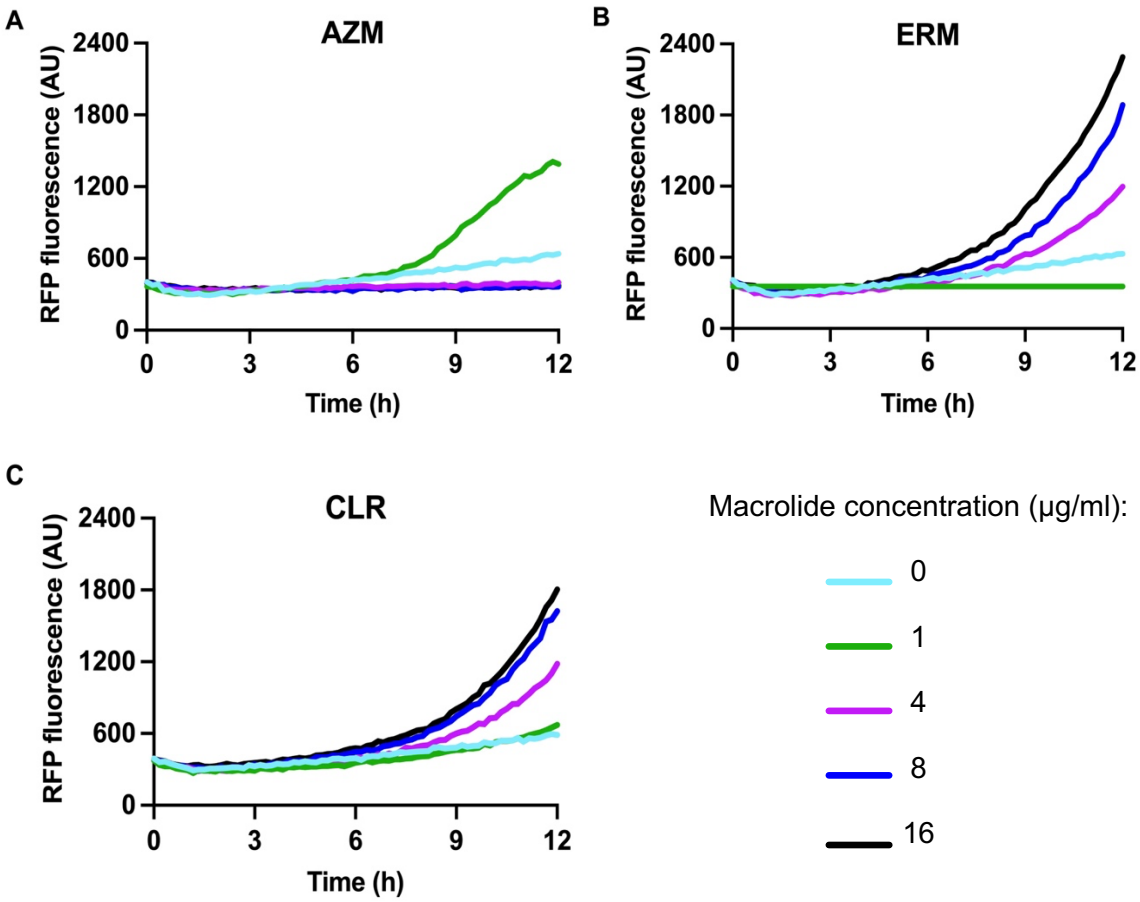

Figure 9. Induction of the RFP fluorescence in bacteria bearing pZb-ALCL-RFP reporter plasmid by macrolides. The expression of the RFP reporter gene in pZb-ALCL-RFP plasmid is induced with azithromycin (**A**), erythromycin (**B**), and clarithromycin (**C**) in Ca-MHB medium at pH 7.4. Fluorescence intensity was measured in 10-minute intervals within 12 hours using microplate reader. The Y-axis represents the intensity of the fluorescence in arbitrary units (AU).

On the other hand, pZb-ErmCL-GFP displayed a much stronger fluorescence signal when induced with macrolides in HEPES-buffered Ca-MHB (pH 7.4). The maximum green fluorescence intensity differed for each macrolide used for induction. All three macrolides of interest successfully induced the GFP reporter gene. However, maximum fluorescence was observed at MIC/4, MIC/16, and MIC/32 for azithromycin, clarithromycin, and erythromycin, respectively (**Figure 10**). While an adequate concentration of macrolides is crucial for the induction of translation, concentrations close to the MIC value will impede protein synthesis. Therefore, the concentration of detectable macrolides with these reporters should be

high enough to induce translation without inhibiting protein synthesis. For instance, the fluorescent signal of GFP was severely diminished in the presence of a concentration range of azithromycin above the MIC due to protein synthesis inhibition.

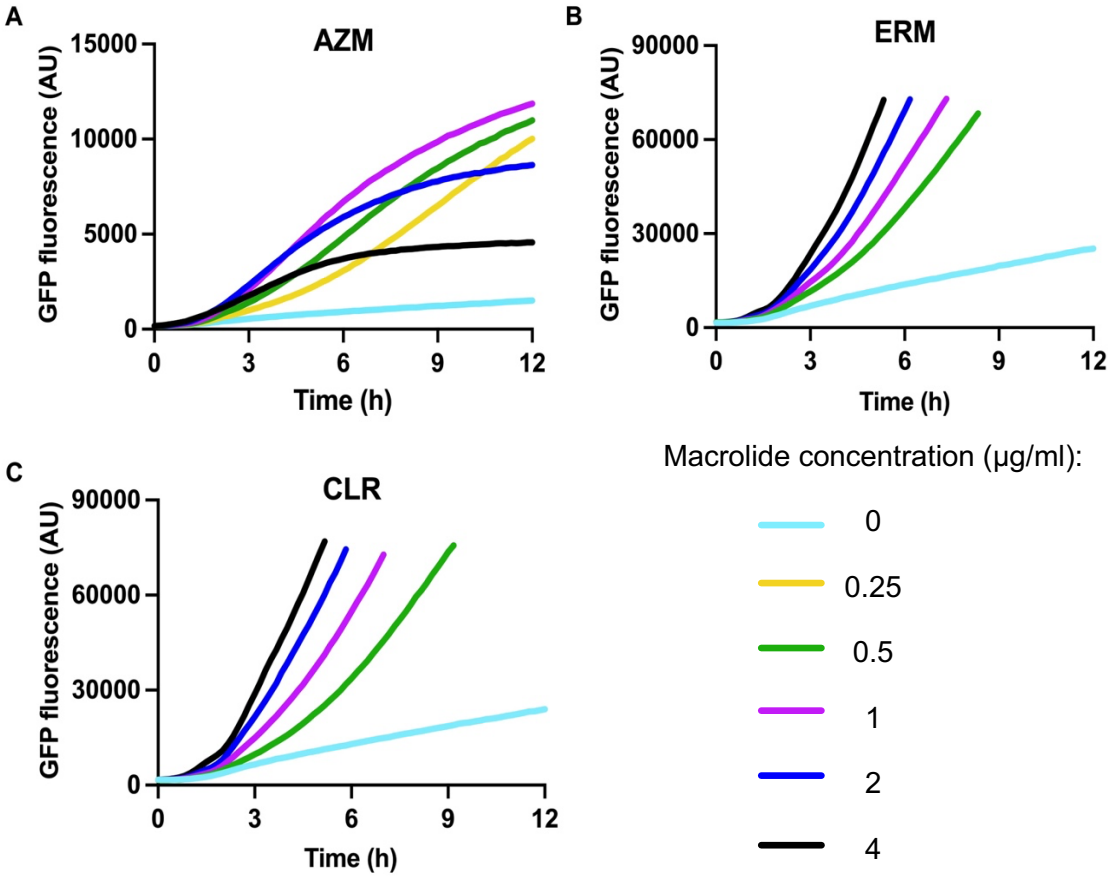

Figure 10. Induction of the GFP fluorescence in bacteria bearing pZb-ErmCL-GFP reporter plasmid by macrolides. The expression of the GFP reporter gene in pZb-ErmCL-GFP plasmid is induced with azithromycin (**A**), erythromycin (**B**), and clarithromycin (**C**) in Ca-MHB medium at pH 7.4. Fluorescence intensity was measured in 10-minute intervals within 12 hours using microplate reader. The Y-axis represents the intensity of the fluorescence in arbitrary units (AU).

Moreover, a strong red fluorescent signal was observed following the induction of pZb-ErmCL-KAT with macrolides (**Figure 11**). While both pZb-ErmCL-GFP and pZb-ErmCL-KAT managed to detect the macrolide concentrations below the MIC in Ca-MHB successfully, the KAT fluorescence signal tended to accumulate much slower than that of GFP (**Figure 10**). Consequently, pZb-ErmCL-GFP was selected as the optimal reporter to be proceeded with due to its efficacy in reporting all three macrolides tested.

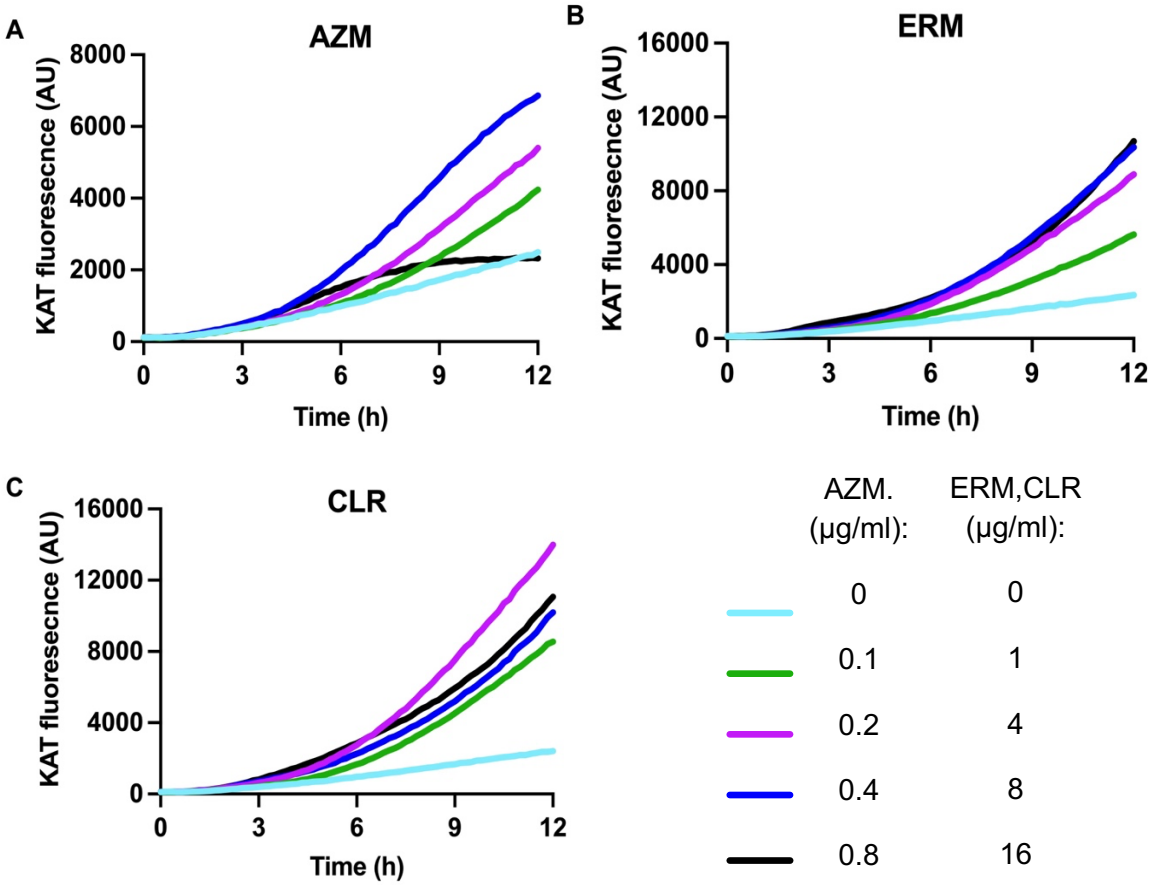

Figure 11. Induction of the KAT fluorescence in bacteria bearing pZb-ErmCL-KAT reporter plasmid by macrolides. The expression of the KAT reporter gene in pZb-ErmCL-KAT plasmid is induced with azithromycin (**A**), erythromycin (**B**), and clarithromycin (**C**) in Ca-MHB medium at pH 7.4. Fluorescence intensity was measured in 10-minute intervals within 12 hours using microplate reader. The Y-axis represents the intensity of the fluorescence in arbitrary units (AU).

Even though Ca-MHB is a standard medium for testing antibiotic sensitivity, it does not resemble the intracellular environment of bacteria within the host cell. Thus, the expression of GFP and KAT reporters was further examined in MES-buffered LPM medium (pH 5.5), which allows for a similar environment to that of acidic intracellular vacuoles or phagosomes where the reporters are aimed to be used. A drastic reduction was noted in the intensity of the fluorescence signal in both fluorescent reporters compared to neutral pH (data not shown). Previous studies have also underlined the downgrading effect of low pH on GFP fluorescence. The pH sensitivity is indeed among the main limiting factors in the utilization of GFP as a quantitative tool to study acidic intracellular compartments such as vacuoles.

The susceptibility of all GFPs to pH can be ascribed to the protonation of the light-absorbing part of the chromophore, which is electron-rich (Shaner et al., 2007). However, when the MIC data is taken into account, it can be concluded that the reduction in GFP reporter expression, in this case, is not a consequence of pH sensitivity but merely due to the inability of the macrolide to penetrate the bacterial cell and subsequently induce the translation of GFP reporter gene. This hypothesis needed to be tested further. To do so, we tested the expression of another GFP reporter that is not preceded by a regulatory leader peptide ORF at pH 7.4 and 5.5 in both Ca-MHB and LPM media. The absence of the leader peptide implies that the expression of GFP is not dependent on the presence of a macrolide, allowing us to solely monitor the effect of pH on GFP fluorescence (**Figure 12**). The results attained indicate that the impact of low pH on GFP fluorescence is relatively minor and, thus, does not explain the drastic reduction observed in the case of pZb-ErmCL-GFP reporter plasmid. Therefore, the effect of antibiotic drug accumulation in the bacterial cells on low pZb-ErmCL-GFP signal is more significant than the potential effect of acidic pH.

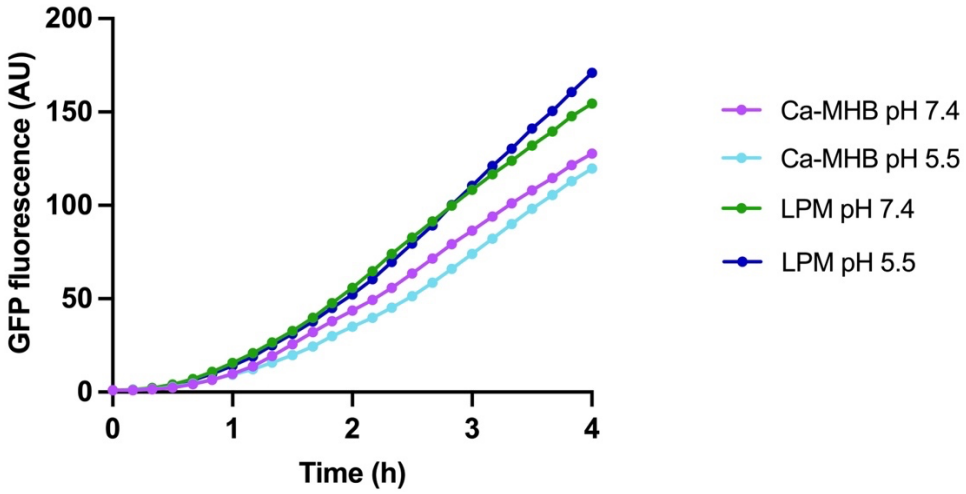

Figure 12. The effect of pH on GFP expression in reporter plasmid without leader peptide. The fluorescence intensity of GFP was measured at pH 5.5 and 7.4 in both Ca-MHB and LPM medium over 4 hours using the microtiter plate reader. The figure indicates that the difference in fluorescence intensity between the two pH conditions is relatively minor. The Y-axis represents the intensity of the fluorescence in arbitrary units (AU).

3.2.4 Reporter gene expression can be induced by certain macrolides on solid medium

The induction of GFP and KAT fluorescence in bacteria bearing pZb-ErmCL-GFP or pZb-ErmCL-KAT reporter plasmids was further tested by various macrolides on MOPS and LPM

plates. Preliminary results indicate that the reporter plasmids can only report the three macrolides that were also tested on the 96-well microtiter plate: azithromycin, erythromycin, and clarithromycin (**Figure 13**). In addition, no significant induction was perceived in the LPM medium compared to MOPS. A strong background fluorescence was exhibited in LPM plates which may be due to the Casamino acid content. Therefore, while this assay was informative regarding the efficacy of various macrolides, it serves problems such as background fluorescence in media as well as on paper discs.

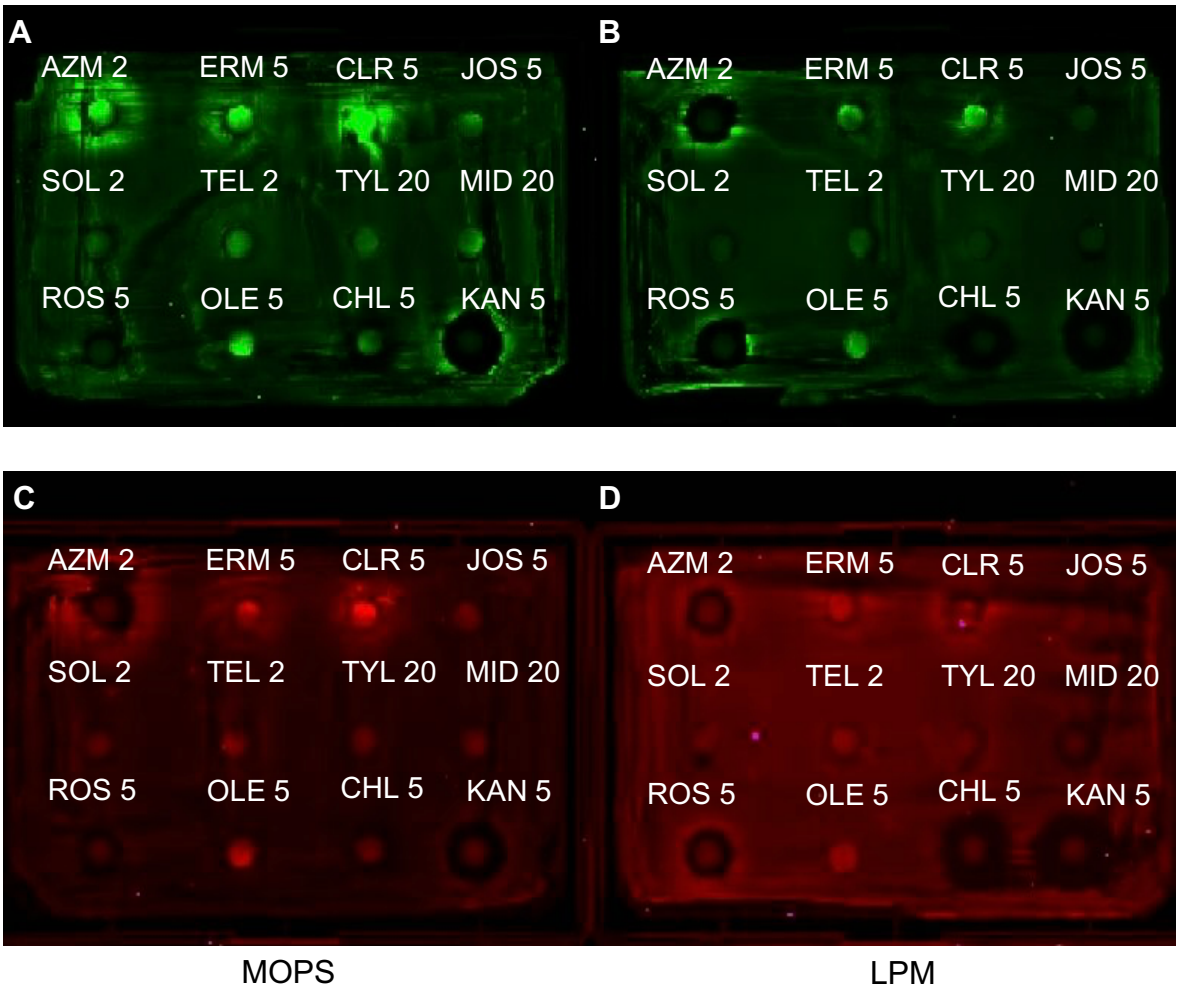

Figure 13. GFP and KAT fluorescence in bacteria bearing pZb-ErmCL-GFP and pZb-ErmCL-KAT plasmids on solid medium. The fluorescence of GFP was induced with 10 macrolides on MOPS (**A**) and LPM (**B**) plates. Similarly, the expression of KAT was induced with the same macrolides on MOPS (**C**) and LPM (**D**) plates. The antibiotics are depicted in the figure, and each number next to the antibiotic's abbreviation corresponds to the amount of drug in µg. Chloramphenicol and kanamycin were utilized as negative control.

3.2.5 GFP expression in individual bacteria is dependent on azithromycin concentration

Flow cytometry was carried out to assess the expression of GFP at the single-cell level. The expression of GFP reporter in pZb-ErmCL-GFP was induced with AZM in Ca-MHB pH 7.4, and the fluorescence intensity at different macrolide concentrations was measured at three different time points (**Figure 14**). Prior to flow cytometry, the cells were stained with FM™ 4-64 dye which stains the bacterial cell membrane.

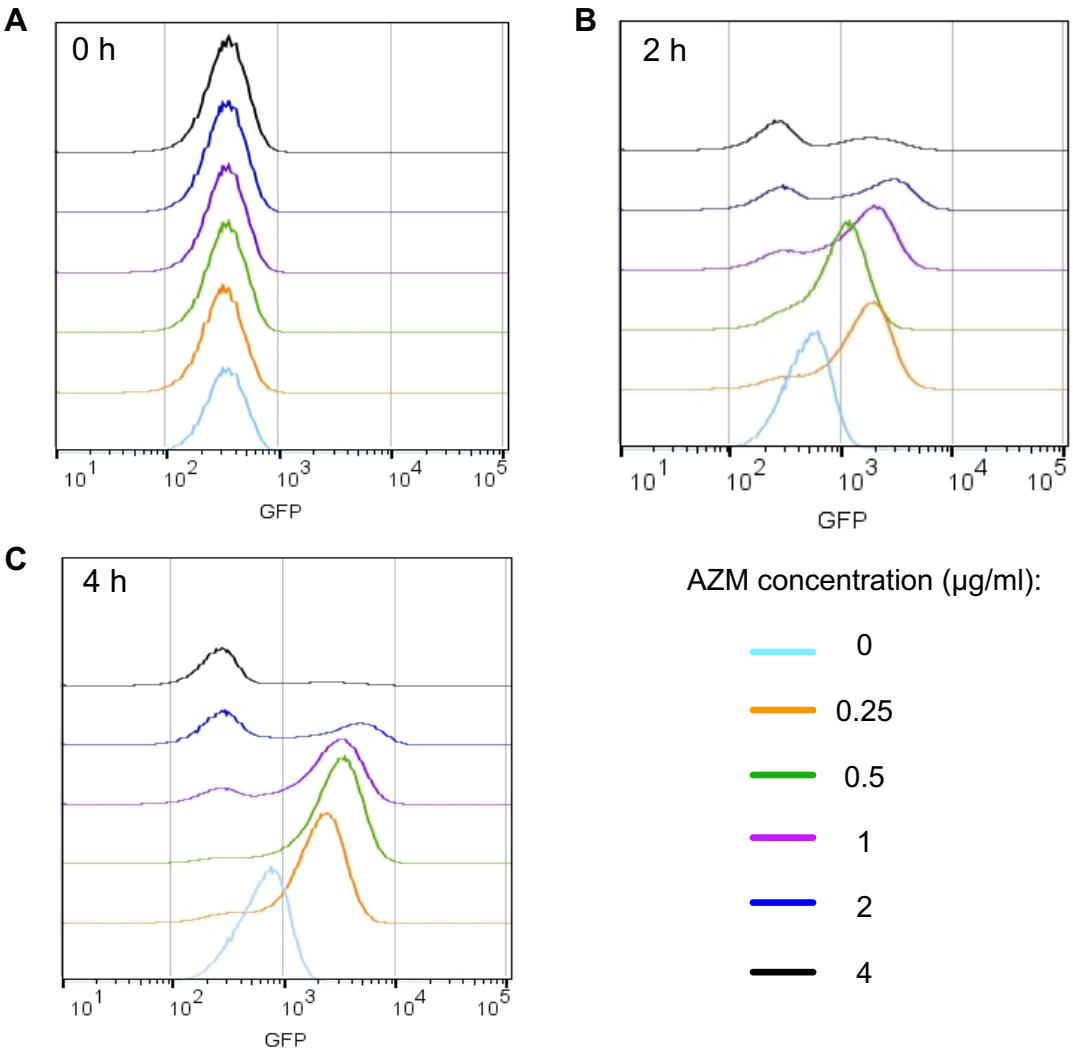

Figure 14. GFP fluorescence intensity in *E. coli* CFT073 cells. The fluorescence intensity of GFP was measured at three time points: prior to the addition of azithromycin (**A**), two hours (**B**) and 4 hours (**C**) after induction. The histograms indicate the number of events detected at different GFP fluorescence levels.

It was observed that azithromycin concentrations below MIC induced GFP expression over time in a concentration-dependent manner. However, a subpopulation of dim cells appeared at higher concentrations (1 μg/ml and above). Moreover, the fraction of dim cells increased during incubation, indicating that some of the bacteria that exhibited GFP signal at 2 hours timepoint had lost the green fluorescence by the 4 hours timepoint. The heterogeneity observed in flow cytometry raised the question of why a subpopulation of cells is not expressing GFP. This may be attributed to four factors: 1) Inability of azithromycin to permeate the bacterial cell, 2) Inability of azithromycin to accumulate inside the cell due to the activity of efflux pumps, 3) Protein synthesis inhibition due to high levels of azithromycin within the bacterial cell, and 4) Leakage of GFP out of dead bacterial cells. To further investigate the results observed in flow cytometry data and characterize the dim events, an L-arabinose inducible reporter plasmid derived from pBAD33 with mScarlet reporter gene was constructed (pBAD33-mScarlet). Both reporter plasmids (pZb-ErmCL-GFP and pBAD33-mScarlet) were transformed into *E. coli* CFT073 strain. We aimed to utilize the expression of the second reporter, mScarlet, to distinguish whether the dim events perceived in the preliminary results were due to a lack of induction or azithromycin's inhibitory effect on protein synthesis. If the latter is the case, we would expect to see cells that do not express neither GFP nor mScarlet. The results indicated that not all GFP expressing cells expressed mScarlet, and the dim subpopulation of GFP was still present at higher azithromycin concentrations (**Figure 15**). Additionally, these dim cells did not demonstrate any mScarlet fluorescence. This leads to the conclusion that the emergence of the dim subpopulation may be a consequence of either protein synthesis inhibition by high concentrations of azithromycin or merely due to the presence of dead bacteria.

Furthermore, mScarlet was induced by L-arabinose in only a fraction of cells. Hence, pBAD33-mScarlet is not an optimal reporter plasmid for protein synthesis.

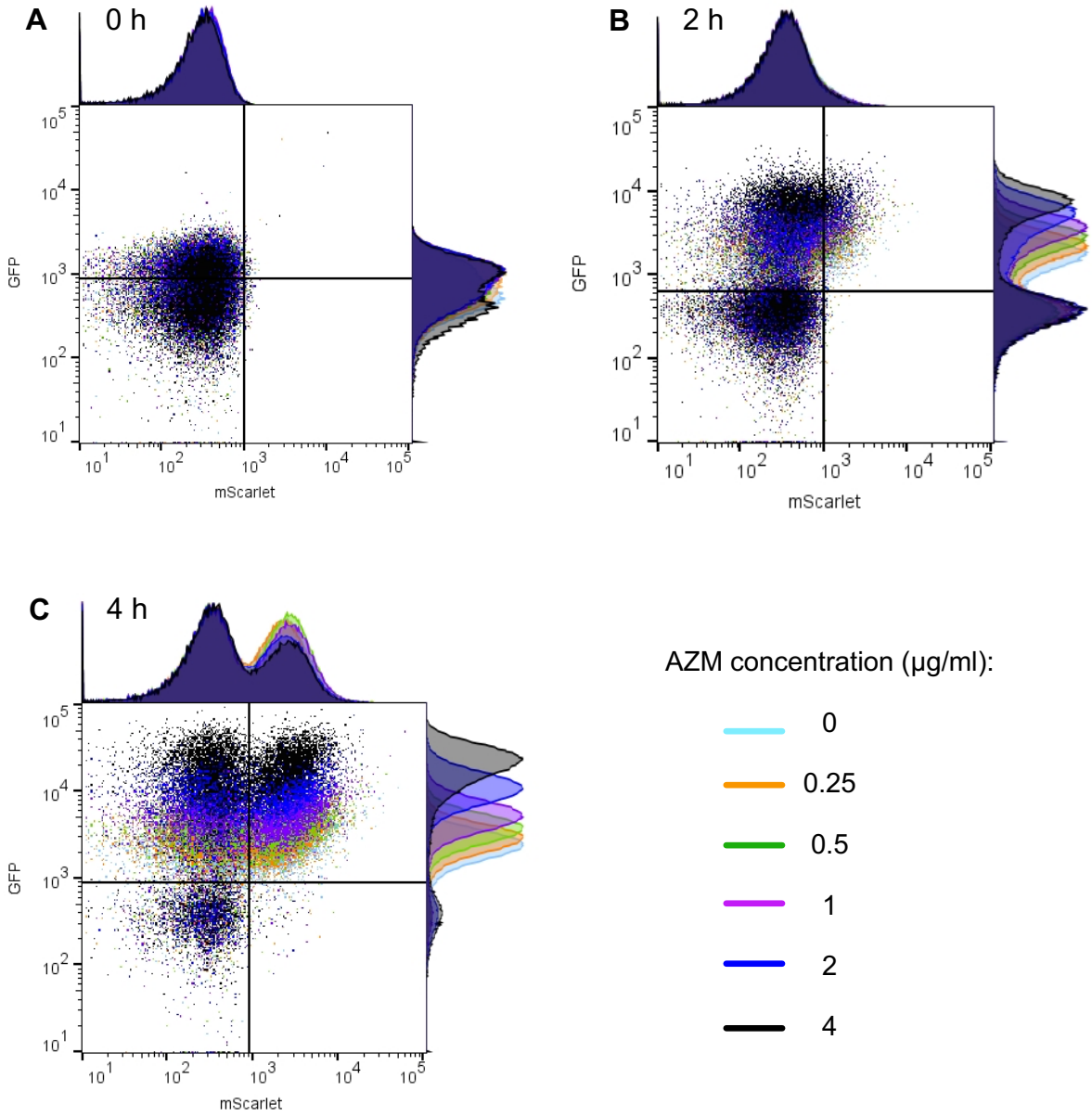

Figure 15. GFP and mScarlet fluorescence intensity in *E. coli* CFT073 cells. The fluorescence intensity of GFP and mScarlet measured at three time points after addition of different AZM concentrations and 0.2% L-arabinose: pre-incubation (**A**), two hours after incubation (**B**) , and 4 hours after incubation (**C**). Each point on the dot plot indicates an event detected. The histograms indicate the number of events detected at different GFP and mScarlet fluorescence levels.

Ultimately, to be able to examine the reporters in infection models in future experiments, dual reporter plasmid pSC101-ErmCL-GFP-mScarlet was constructed by inserting the

ErmCL leader peptide encoding sequence and two reporter genes under a constitutive promoter. However, no GFP or mScarlet fluorescence was perceived in flow cytometry, implying the failure of the dual reporter in detecting azithromycin *in vitro*.

In conclusion, we observed that the reporter was expressed in an azithromycin concentration-dependent manner in individual bacteria, but not in all bacterial cells. At higher azithromycin concentrations, a subpopulation of dim cells emerged. Further experiments are required to detect whether the dim cells were merely dead or protein synthesis was inhibited within them by azithromycin.

SUMMARY

Macrolide antibiotics have long been associated with the treatment of infections caused by Gram-positive bacteria. On the other hand, treatment with azithromycin has proven to be highly effective against *Salmonella*, which is a Gram-negative bacterium. Previous studies indicate that the maximum achievable plasma concentration for Azithromycin (0.5 µg/ml) is noticeably lower than the published MIC values, which are in the 4-8 µg/ml range. However, it is important to note that MIC measurements are carried out in standard conditions that do not correspond to the conditions in infection sites. Numerous factors contribute to differences between the standard media conditions and infection sites which alter the minimum inhibitory concentration of antibiotics and, thus, the efficacy of treatment. Among these factors are pH, magnesium and phosphate content, and antimicrobial peptides. Intracellular bacteria such as *Salmonella* and uropathogenic *E. coli* typically proliferate within acidified vacuoles or phagosomes inside the host cell, in an environment with lower pH than standard laboratory media. Moreover, low magnesium and phosphate levels at the infection sites lead to a reduction in the stability of the lipopolysaccharide layer of the outer membrane, thereby increasing its permeability to hydrophobic antimicrobial drugs. The antimicrobial peptides present at the infection site also play a role in permeabilizing the bacterial membrane, hence increasing the efficacy of antibiotic treatment at lower drug doses.

In this study, we investigated the potential efficiency of azithromycin against Gram-negative uropathogenic *E. coli*. The activity of azithromycin against uropathogenic *E. coli* was tested in a standard testing medium as well as conditions that resemble the infection site. In order to mimic the infection site, we determined the MIC of azithromycin in a medium with acidic pH and low phosphate and magnesium content. The MIC increased drastically in acidic pH. However, when the infection-mimicking media were tested at neutral pH, the MICs got close to the maximal plasma concentration. Further reduction was observed in MIC values upon the addition of permeabilizing peptide and efflux pump inhibitor. This suggests that the effect of azithromycin on bacteria can differ depending on the cellular compartment in which they reside within the host cell.

Fluorescent bioreporters are promising tools for measuring antibiotic concentrations within *in vitro* and *in vivo* infection models. In this work, we aimed to validate the use of four fluorescent reporter plasmids (pZb-ErmCL-RFP, pZb-ALCL-RFP, pZb-ErmCL-GFP, pZb-ErmCL-KAT) in detecting macrolide antibiotics, primarily azithromycin. First and foremost, each reporter was tested against azithromycin, erythromycin, and clarithromycin in Ca-

MHB. Our preliminary results indicate that RFP-based reporters are inefficient in detecting macrolides. Further experiments were carried out to test pZb-ErmCL-GFP and pZb-ErmCL-KAT, leading to the conclusion that the GFP-based reporter can detect azithromycin, erythromycin, and clarithromycin concentrations below MIC.

Flow cytometry data showed that the induction of the GFP reporter gene by azithromycin is dependent on the drug concentration. On the other hand, azithromycin concentrations close to MIC give rise to the emergence of a dim subpopulation of cells that do not demonstrate any fluorescence.

To conclude, the results encourage us to test azithromycin against various Gram-negative pathogens in further trials. While GFP and KAT-based reporters are propitious tools to be utilized in future experiments, further development is required for the reporters to make them compatible with infection models.

REFERENCES

Aktar, A., Wodz, K. M., & Heit, B. (2022). *Monitoring Cellular Responses to Infection with Fluorescent Biosensors* (pp. 99–114). https://doi.org/10.1007/978-1-0716-2051-9_6

Al-Marzooq, F., Ghazawi, A., Tariq, S., Daoud, L., & Collyns, T. (2022a). Discerning the role of polymyxin B nonapeptide in restoring the antibacterial activity of azithromycin against antibiotic-resistant Escherichia coli. *Frontiers in Microbiology*, *13*. https://doi.org/10.3389/fmicb.2022.998671

Al-Marzooq, F., Ghazawi, A., Tariq, S., Daoud, L., & Collyns, T. (2022b). Discerning the role of polymyxin B nonapeptide in restoring the antibacterial activity of azithromycin against antibiotic-resistant Escherichia coli. *Frontiers in Microbiology*, *13*. https://doi.org/10.3389/fmicb.2022.998671

Amsden, G. W. (2005). Anti-inflammatory effects of macrolides—an underappreciated benefit in the treatment of community-acquired respiratory tract infections and chronic inflammatory pulmonary conditions? *Journal of Antimicrobial Chemotherapy*, *55*(1), 10–21. https://doi.org/10.1093/jac/dkh519

Ashima K. Bhardwaj, & Priyabrata Mohanty. (2012). Bacterial Efflux Pumps Involved in Multidrug Resistance and their Inhibitors: Rejuvinating the Antimicrobial Chemotherapy. *Recent Patents on Anti-Infective Drug Discovery*, *7*(1), 73–89. https://doi.org/10.2174/157489112799829710

Balaban, N. Q., Gerdes, K., Lewis, K., & McKinney, J. D. (2013). A problem of persistence: still more questions than answers? *Nature Reviews Microbiology*, *11*(8), 587–591. https://doi.org/10.1038/nrmicro3076

Brown, E. D., & Wright, G. D. (2016). Antibacterial drug discovery in the resistance era. In *Nature* (Vol. 529, Issue 7586, pp. 336–343). Nature Publishing Group. https://doi.org/10.1038/nature17042

Cambré, A., & Aertsen, A. (2020). Bacterial Vivisection: How Fluorescence-Based Imaging Techniques Shed a Light on the Inner Workings of Bacteria. *Microbiology and Molecular Biology Reviews*, *84*(4). https://doi.org/10.1128/MMBR.00008-20

Chalfie, M., Tu, Y., Euskirchen, G., Ward, W. W., & Prasher, D. C. (1994). Green Fluorescent Protein as a Marker for Gene Expression. *Science*, *263*(5148), 802–805. https://doi.org/10.1126/science.8303295

Champney, W. S., & Burdine, R. (1995). Macrolide antibiotics inhibit 50S ribosomal subunit assembly in Bacillus subtilis and Staphylococcus aureus. *Antimicrobial Agents and Chemotherapy*, *39*(9), 2141–2144. https://doi.org/10.1128/AAC.39.9.2141

Cho, H., Uehara, T., & Bernhardt, T. G. (2014). Beta-Lactam Antibiotics Induce a Lethal Malfunctioning of the Bacterial Cell Wall Synthesis Machinery. *Cell*, *159*(6), 1300–1311. https://doi.org/10.1016/j.cell.2014.11.017

Coates, A., Hu, Y., Bax, R., & Page, C. (2002). The future challenges facing the development of new antimicrobial drugs. *Nature Reviews Drug Discovery*, *1*(11), 895–910. https://doi.org/10.1038/nrd940

Coombes, B. K., Brown, N. F., Valdez, Y., Brumell, J. H., & Finlay, B. B. (2004). Expression and Secretion of Salmonella Pathogenicity Island-2 Virulence Genes in Response to Acidification Exhibit Differential Requirements of a Functional Type III Secretion Apparatus and SsaL. *Journal of Biological Chemistry*, *279*(48), 49804–49815. https://doi.org/10.1074/jbc.M404299200

Dalhoff, A., Schubert, S., & Ullmann, U. (2005). Effect of pH on the in Vitro Activity of and Propensity for Emergence of Resistance to Fluoroquinolones, Macrolides, and a Ketolide. *Infection*, *33*(S2), 36–43. https://doi.org/10.1007/s15010-005-8206-y

Fisher, R. A., Gollan, B., & Helaine, S. (2017). Persistent bacterial infections and persister cells. *Nature Reviews Microbiology*, *15*(8), 453–464. https://doi.org/10.1038/nrmicro.2017.42

Gaynor, M., & Mankin, A. (2005). Macrolide Antibiotics: Binding Site, Mechanism of Action, Resistance. *Current Topics in Medicinal Chemistry*, *3*(9), 949–960. https://doi.org/10.2174/1568026033452159

Gollan, B., Grabe, G., Michaux, C., & Helaine, S. (2019). Bacterial Persisters and Infection: Past, Present, and Progressing. *Annual Review of Microbiology*, *73*(1), 359–385. https://doi.org/10.1146/annurev-micro-020518-115650

Gonçalves-Pereira, J., & Póvoa, P. (2011). Antibiotics in critically ill patients: a systematic review of the pharmacokinetics of β-lactams. *Critical Care*, *15*(5), R206. https://doi.org/10.1186/cc10441

Gotuzzo, E., Morris, J. G., Benavente, L., Wood, P. K., Levine, O., Black, R. E., & Levine, M. M. (1987). Association between specific plasmids and relapse in typhoid fever. *Journal of Clinical Microbiology*, *25*(9), 1779–1781. https://doi.org/10.1128/jcm.25.9.1779-1781.1987

Guzman, L. M., Belin, D., Carson, M. J., & Beckwith, J. (1995). Tight regulation, modulation, and high-level expression by vectors containing the arabinose PBAD promoter. *Journal of Bacteriology*, *177*(14), 4121–4130. https://doi.org/10.1128/jb.177.14.4121-4130.1995

Hansen, L. H., Ferrari, B., Sørensen, A. H., Veal, D., & Sørensen, S. J. (2001). Detection of Oxytetracycline Production by *Streptomyces rimosus* in Soil Microcosms by Combining Whole-Cell Biosensors and Flow Cytometry. *Applied and Environmental Microbiology*, *67*(1), 239–244. https://doi.org/10.1128/AEM.67.1.239-244.2001

Helaine, S., & Holden, D. W. (2013). Heterogeneity of intracellular replication of bacterial pathogens. *Current Opinion in Microbiology*, *16*(2), 184–191. https://doi.org/10.1016/j.mib.2012.12.004

Joyner, D. C., & Lindow, S. E. (2000). Heterogeneity of iron bioavailability on plants assessed with a whole-cell GFP-based bacterial biosensor. *Microbiology*, *146*(10), 2435–2445. https://doi.org/10.1099/00221287-146-10-2435

Kamaruzzaman, N. F., Kendall, S., & Good, L. (2017). Targeting the hard to reach: challenges and novel strategies in the treatment of intracellular bacterial infections. *British Journal of Pharmacology*, *174*(14), 2225–2236. https://doi.org/10.1111/bph.13664

Kannan, K., Kanabar, P., Schryer, D., Florin, T., Oh, E., Bahroos, N., Tenson, T., Weissman, J. S., & Mankin, A. S. (2014). The general mode of translation inhibition by macrolide antibiotics. *Proceedings of the National Academy of Sciences of the United States of America*, *111*(45), 15958–15963. https://doi.org/10.1073/pnas.1417334111

Kim, J. J., & Sundin, G. W. (2000). Regulation of the *rulAB* Mutagenic DNA Repair Operon of *Pseudomonas syringae* by UV-B (290 to 320 Nanometers) Radiation and Analysis

of *rulAB* -Mediated Mutability In Vitro and In Planta. *Journal of Bacteriology*, *182*(21), 6137–6144. https://doi.org/10.1128/JB.182.21.6137-6144.2000

Leveau, J. H. J., & Lindow, S. E. (2002). Bioreporters in microbial ecology. *Current Opinion in Microbiology*, *5*(3), 259–265. https://doi.org/10.1016/S1369-5274(02)00321-1

Lin, L., Nonejuie, P., Munguia, J., Hollands, A., Olson, J., Dam, Q., Kumaraswamy, M., Rivera, H., Corriden, R., Rohde, M., Hensler, M. E., Burkart, M. D., Pogliano, J., Sakoulas, G., & Nizet, V. (2015). Azithromycin Synergizes with Cationic Antimicrobial Peptides to Exert Bactericidal and Therapeutic Activity Against Highly Multidrug-Resistant Gram-Negative Bacterial Pathogens. *EBioMedicine*, *2*(7), 690–698. https://doi.org/10.1016/j.ebiom.2015.05.021

Mao, J. C. H., & Robishaw, E. E. (1972). Erythromycin, a peptidyltransferase effector. *Biochemistry*, *11*(25), 4864–4872. https://doi.org/10.1021/bi00775a035

Masi, M., Réfregiers, M., Pos, K. M., & Pagès, J.-M. (2017). Mechanisms of envelope permeability and antibiotic influx and efflux in Gram-negative bacteria. *Nature Microbiology*, *2*(3), 17001. https://doi.org/10.1038/nmicrobiol.2017.1

Matzneller, P., Krasniqi, S., Kinzig, M., Sörgel, F., Hüttner, S., Lackner, E., Müller, M., & Zeitlinger, M. (2013). Blood, Tissue, and Intracellular Concentrations of Azithromycin during and after End of Therapy. *Antimicrobial Agents and Chemotherapy*, *57*(4), 1736–1742. https://doi.org/10.1128/AAC.02011-12

Melander, R. J., Zurawski, D. V., & Melander, C. (2018). Narrow-spectrum antibacterial agents. *MedChemComm*, *9*(1), 12–21. https://doi.org/10.1039/C7MD00528H

Menninger, J. R., & Otto, D. P. (1982). Erythromycin, carbomycin, and spiramycin inhibit protein synthesis by stimulating the dissociation of peptidyl-tRNA from ribosomes. *Antimicrobial Agents and Chemotherapy*, *21*(5), 811–818. https://doi.org/10.1128/AAC.21.5.811

Miller, W. G., Brandl, M. T., Quiñones, B., & Lindow, S. E. (2001). Biological sensor for sucrose availability: relative sensitivities of various reporter genes. *Applied and Environmental Microbiology*, *67*(3), 1308–1317. https://doi.org/10.1128/AEM.67.3.1308-1317.2001

Murata, T., Tseng, W., Guina, T., Miller, S. I., & Nikaido, H. (2007). PhoPQ-Mediated Regulation Produces a More Robust Permeability Barrier in the Outer Membrane of *Salmonella enterica* Serovar Typhimurium. *Journal of Bacteriology*, *189*(20), 7213–7222. https://doi.org/10.1128/JB.00973-07

Neidhardt, F. C., Bloch, P. L., & Smith, D. F. (1974). Culture Medium for Enterobacteria. *Journal of Bacteriology*, *119*(3), 736–747. https://doi.org/10.1128/jb.119.3.736-747.1974

Norris, S. J. (2006). Antigenic variation with a twist - the Borrelia story. *Molecular Microbiology*, *60*(6), 1319–1322. https://doi.org/10.1111/j.1365-2958.2006.05204.x

Prajapati, J. D., Kleinekathöfer, U., & Winterhalter, M. (2021). How to Enter a Bacterium: Bacterial Porins and the Permeation of Antibiotics. *Chemical Reviews*, *121*(9), 5158–5192. https://doi.org/10.1021/acs.chemrev.0c01213

Quan, J., & Tian, J. (2009). Circular Polymerase Extension Cloning of Complex Gene Libraries and Pathways. *PLoS ONE*, *4*(7), e6441. https://doi.org/10.1371/journal.pone.0006441

Rathman, M., Sjaastad, M. D., & Falkow, S. (1996). Acidification of phagosomes containing Salmonella typhimurium in murine macrophages. *Infection and Immunity*, *64*(7), 2765–2773. https://doi.org/10.1128/iai.64.7.2765-2773.1996

Roostalu, J., Jõers, A., Luidalepp, H., Kaldalu, N., & Tenson, T. (2008). Cell division in Escherichia colicultures monitored at single cell resolution. *BMC Microbiology*, *8*(1), 68. https://doi.org/10.1186/1471-2180-8-68

Shaner, N. C., Patterson, G. H., & Davidson, M. W. (2007). Advances in fluorescent protein technology. *Journal of Cell Science*, *120*(24), 4247–4260. https://doi.org/10.1242/jcs.005801

Sharma, A., Gupta, V., & Pathania, R. (2019). Efflux pump inhibitors for bacterial pathogens: From bench to bedside. *Indian Journal of Medical Research*, *149*(2), 129. https://doi.org/10.4103/ijmr.IJMR_2079_17

Shcherbo, D., Merzlyak, E. M., Chepurnykh, T. V, Fradkov, A. F., Ermakova, G. V, Solovieva, E. A., Lukyanov, K. A., Bogdanova, E. A., Zaraisky, A. G., Lukyanov, S.,

& Chudakov, D. M. (2007). Bright far-red fluorescent protein for whole-body imaging. *Nature Methods*, *4*(9), 741–746. https://doi.org/10.1038/nmeth1083

Tsubery, H., Ofek, I., Cohen, S., & Fridkin, M. (2000). The Functional Association of Polymyxin B with Bacterial Lipopolysaccharide Is Stereospecific: Studies on Polymyxin B Nonapeptide. *Biochemistry*, *39*(39), 11837–11844. https://doi.org/10.1021/bi000386q

Tulkens, P. M. (1991). Intracellular distribution and activity of antibiotics. *European Journal of Clinical Microbiology & Infectious Diseases*, *10*(2), 100–106. https://doi.org/10.1007/BF01964420

Vaara, M., & Viljanen, P. (1985). Binding of polymyxin B nonapeptide to gram-negative bacteria. *Antimicrobial Agents and Chemotherapy*, *27*(4), 548–554. https://doi.org/10.1128/AAC.27.4.548

Vázquez-Laslop, N., & Mankin, A. S. (2018). How Macrolide Antibiotics Work. In *Trends in Biochemical Sciences* (Vol. 43, Issue 9, pp. 668–684). Elsevier Ltd. https://doi.org/10.1016/j.tibs.2018.06.011

Weisblum, B. (1998). Macrolide resistance. *Drug Resistance Updates*, *1*(1), 29–41. https://doi.org/10.1016/S1368-7646(98)80212-4

Zhu, Y., Elcin, E., Jiang, M., Li, B., Wang, H., Zhang, X., & Wang, Z. (2022). Use of whole-cell bioreporters to assess bioavailability of contaminants in aquatic systems. *Frontiers in Chemistry*, *10*, 1018124. https://doi.org/10.3389/fchem.2022.1018124

NON-EXCLUSIVE LICENCE TO REPRODUCE THESIS AND MAKE THESIS PUBLIC

I, Ana Shahpazir,

1. grant the University of Tartu a free permit (non-exclusive licence) to reproduce, for the purpose of preservation, including for adding to the DSpace digital archives until the expiry of the term of copyright, my thesis

"Activity of macrolides against uropathogenic Escherichia coli",

supervised by Niilo Kaldalu.

2. I grant the University of Tartu the permit to make the thesis specified in point 1 available to the public via the web environment of the University of Tartu, including via the DSpace digital archives, under the Creative Commons licence CC BY NC ND 4.0, which allows, by giving appropriate credit to the author, to reproduce, distribute the work and communicate it to the public, and prohibits the creation of derivative works and any commercial use of the work from ***24/05/2026*** until the expiry of the term of copyright,
3. I am aware that the author retains the rights specified in points 1 and 2.

4. I confirm that granting the non-exclusive licence does not infringe other persons' intel. lectual property rights or rights arising from the personal data protection legislation.

Ana Shahpazir

24/05/2023